NASA Technical Memorandum 88943

Measurement Uncertainty for the Uniform Engine Testing Program Conducted at NASA Lewis Research Center

Mahmood Abdelwahab and Thomas J. Biesiadny
Lewis Research Center
Cleveland, Ohio

and

Dean Silver
Air Force Systems Command Liaison Office
Lewis Research Center
Cleveland, Ohio

May 1987

NASA

MEASUREMENT UNCERTAINTY FOR THE UNIFORM ENGINE TESTING PROGRAM CONDUCTED AT NASA LEWIS RESEARCH CENTER

Mahmood Abdelwahab and Thomas J. Biesiadny
National Aeronautics and Space Administration
Lewis Research Center
Cleveland, Ohio 44135

and

Dean Silver
Air Force Systems Command Liaison Office
Lewis Research Center
Cleveland, Ohio 44135

SUMMARY

An uncertainty analysis was conducted to determine the bias and precision errors and total uncertainty of measured turbojet engine performance parameters. The engine tests were conducted as part of the Uniform Engine Test Program which was sponsored by the Advisory Group for Aerospace Research and Development (AGARD). With the same engines, support hardware, and instrumentation, performance parameters were measured twice, once during tests conducted in test cell number 3 and again during tests conducted in test cell number 4 of the NASA Lewis Propulsion Systems Laboratory. The analysis covers 15 engine parameters, including engine inlet airflow, engine net thrust, and engine specific fuel consumption measured at high rotor speed of 8875 rpm. Measurements were taken at three flight conditions defined by the following engine inlet pressure, engine inlet total temperature, and engine ram ratio: (1) 82.7 kPa, 288 K, 1.0, (2) 82.7 kPa, 288 K, 1.3, and (3) 20.7 kPa, 288 K, 1.3.

In terms of bias, precision, and uncertainty magnitudes, there were no differences between most measurements made in test cell numbers 3 and 4. The magnitude of the errors increased for both test cells as engine pressure level decreased. Also, the level of the bias error was two to three times larger than that of the precision error.

E-3234

INTRODUCTION

This report presents the NASA Lewis error assessment of the engine performance parameters measured during the Uniform Engine Test Program (UETP) which was conducted in the NASA Lewis Propulsion Systems Laboratory (PSL), in test cell number 3 during 1981, and again, in test cell number 4 during 1985. Errors, in terms of bias, precision, and uncertainty, are presented for selected engine performance parameters measured at a target high rotor speed and three representative test conditions agreed upon by the Working Group sponsoring the UETP. Measurement system descriptions and a comparison of error magnitudes between measurements in cell numbers 3 and 4 are also presented.

The Uniform Engine Testing Program is sponsored by the Propulsion and Energetic Panel, Working Group 15, of the Advisory Group for Aerospace Research and Development (AGARD). The program consists of testing two J57 turbojet engines under identical conditions in a number of altitude and ground level facilities in several NATO Countries (U.S.A., England, France, Canada, and Turkey). The purpose of the program is to compare engine performance measurements made in these various test facilities and to establish the reasons for any observed differences (ref. 1). Several factors can influence the observed measurements. The main ones are as follows: (1) influence of the facility, (2) degradation of engine performance with running time, and (3) facility measurement systems errors. For the NASA Lewis tests, the first two factors were dealt with in references 1 and 2. The purpose of this report is to deal with the third factor by presenting an uncertainty assessment of engine performance parameter measurements made during tests conducted in the NASA Lewis Propulsion Systems Laboratories, test cell numbers 3 and 4.

As agreed upon by the Working Group 15 members, the methodology of error assessment followed in this report is that of reference 3. It assumes that errors fall into two simple classes: bias (or systematic) and precision (or random). A single number representing the limit of error, or total uncertainty is then defined as a combination of the bias and the precision errors. For each class of error, several elemental errors caused by different sources in the measurement process are combined to produce a single value for that class. Sources of elemental errors include calibration, environment, data acquisition, and data reduction. The propagation of each class of error into a performance parameter is then accomplished by using Taylor's series as explained in detail in reference 3.

To provide for a better understanding of the error assessment results, the report will first present a description of the measurement systems and data acquisition systems used in test cell numbers 3 and 4 of PSL. The error results will then be presented as follows: (1) bias, precision, and uncertainty of all measured variables (pressures, temperatures, speeds, areas, forces, and fuel flows); (2) influence coefficients showing the effect of each measured variable on performance parameters; (3) performance parameter biases, precisions, and total uncertainties for measurements made in test cell numbers 3 and 4. The results are presented for three test conditions defined by the following engine inlet pressure, engine inlet temperature, and engine ram ratio: (1) 82.7 kPa, 288 K, 1.0 referred to hereinafter as condition number 3; (2) 82.7 kPa, 288 K, 1.3 referred to hereinafter as condition number 6, (3) 20.7 kPa, 288 K, 1.3 referred to hereinafter as condition number 9.

MEASUREMENT SYSTEMS DESCRIPTION

Six measurement systems were employed during the Uniform Engine Testing Program tests conducted in cells 3 and 4 of the NASA Lewis Propulsion Systems Laboratory. They are force, fuel flow, pressure, temperature, speed, and area. This section will present a brief description of each system and its calibration methods. All systems were the same for cells 3 and 4 except for the pressure system which will be discussed for each cell separately.

Thrust Measurement System

Engine installation. - Figure 1(a) and (b) shows a J57 engine schematic and the instrumentation locations, respectively. A schematic of a typical UETP engine installation in the NASA Lewis Altitude Test Facility is shown in figure 2. The installation was a conventional direct connection. The engine was installed in a "doghouse" test stand mounted on the thrust bed. The bed was suspended by four flexure rods attached to the chamber wall and was free to move except as restrained by a dual load-cell measurement system that allowed the thrust bed to be preloaded.

The test cell included a forward bulkhead which separated the inlet plenum from the test section. Conditioned air flowed from the plenum through the bellmouth into the inlet duct. A labyrinth seal was used to isolate the inlet ducting from the bellmouth which was attached to the forward bulkhead. The inlet ducting, which was mounted on the thrust bed, was mated to the engine through an inflatable seal to minimize loading on the engine front flange. Cell-cooling air was supplied through a manifold supported by the forward bulkhead.

Cell-cooling air and engine exhaust gases were captured by a collector, which extended through the rear bulkhead, thereby minimizing the possibility of exhaust gas recirculation into the test cell.

The two test cells at NASA Lewis where UETP engine tests were conducted, referred to hereinafter as PSL-3 and PSL-4, are of the same physical size - 7.315-m (24-ft) diameter by 11.582-m (39-ft) long. The only difference between the two cells is the distance between the cell center line and the thrust bed, that distance is 3.345 m (6 ft) for PSL-3 and 1.219 m (4 ft) for PSL-4.

Method of calculation. - Net thrust is calculated as follows:

$$FN = FG - WA1 * V_0$$

where

FG gross thrust

V_0 free stream velocity

WA1 airflow rate at station 1

WA1 * V_0 ram drag

(A complete symbol list is given in appendix A.) Gross thrust was calculated by using the steady-state conservation of axial momentum principle: the summation of all axial forces acting on a control volume is zero. This leads to the following equation with the control volume shown in figure 3:

$$FG = FM - FP + F1 + FSEAL + FTARE + FDAP + FD + FBOAT$$

where

ABOAT exhaust nozzle boattail area

ASEAL	labyrinth seal area
AWET	wetted area between plane at start of inlet ducting and plane at station 1
CF	flat plate drag coefficient at zero angle of attack
FBOAT	exhaust nozzle boattail drag force, ABOAT * (PBOAT - PAMB). During all tests PBOAT was made equal to PAMB in the calculations program. Test data show this force to be of negligible magnitude.
FD	force caused by flow on the inside diameter between the labyrinth seal inlet plane and airflow measurement plane: GAM1 * CF * PS1 * M1 * AWET/2
FDAP	force caused by flow through the labyrinth seal and test cell (cooling air), calibrated force
FM	force measured by force load cell, average of two bridges
FP	force measured by preload load cell, average of two bridges
FSEAL	pressure forces acting on the labyrinth seal area, ASEAL * (PSEAL - PAMB)
FTARE	force caused by thrust stand support and service systems, calibrated force
F1	total momentum at inlet plane, WA1 * V1 + A1 * (PS1 - PAMB)
GAM1	specific heat at station 1
M1	Mach number at station 1
PAMB	ambient pressure
PSEAL	average static pressure at station 0.1 and 0.2
PBOAT	average static pressure at station 0.4
PS1	average static pressure at station 1
V1	velocity at station 1

Calibration. - The following calibrations were performed for each engine test program:

(1) Load cells were calibrated against standards traceable to the National Bureau of Standards (NBS). This calibration was performed prior to and after the completion of each UETP entry.

(2) Electrical calibrations of the load cells were performed prior to each test run. Preand post-test run calibration data (zeros and full scales) were recorded at sea level and altitude conditions.

(3) Test stand force calibrations were conducted to determine force (FTARE) caused by thrust stand support and service systems (fuel and instrumentation lines). Calibration procedure consists of applying loads, through the preload system, to the test stand with all service lines pressurized and engine airflow and test cell cooling air off. In equation form

$$FG = FM - FP + \overset{0}{F1} + FTARE + \overset{0}{FDAP} + \overset{0}{FSEAL} + \overset{0}{FD} + \overset{0}{FBOAT}$$

$$\text{and} \quad FTARE = FP - FM$$

where F1, FG, FDAP, FSEAL, FD, and FBOAT are all zero because there is no engine airflow or pressure forces during this calibration. One example of J57 calibration data in PSL-4 is shown in figure 4.

(4) Test facility flow calibrations were conducted to determine force (FDAP) caused by flow through the labyrinth seal and test cell (cooling air). Calibration procedure consists of blanking-off the inlet duct downstream of the labyrinth seal (fig. 5(a)) then pressurizing the duct and flowing air through the seal and test cell (cooling air) and measuring the resultant forces. In equation form

$$FG = FM - FP + \overset{0}{F1} + FTARE + \overset{0}{FDAP} + FSEAL + \overset{0}{FD} + \overset{0}{FBOAT}$$

and

$$FDAP = FP - FM - F1 - FTARE - FSEAL$$

where FG, FD, FBOAT are all zero because there is no engine airflow. Instrumentations used for this calculation (PS1, PSEAL) are shown in figure 5(b) and (c), respectively. An example of J57 calibration data in PSL-4 is shown in figure 6.

Fuel Measurement System

Description. - A schematic of the fuel system is shown in figure 7. Fuel is stored in four 25 000-gal supply tanks. The tanks were located approximately one quarter of a mile from the facility building. Fuel was pumped from the supply tanks to the test facility building. Two stations, one outside the test building and one inside the test cell were available for fuel pressure regulation. A fuel accumulator was installed close to the engine to allow for smoother engine transients.

The facility fuel flow measurement system consists of dual range (high and low range) sets (one set = 2 flow meters) of turbine flow meters and a control valve. The control valve was automated and functioned in the following manner:

(1) Open position: fuel will pass through the high range flow meters only.

(2) Closed position: fuel will pass through the high range and the low range meters.

Method of calculation. - The following equation was used to calculate fuel flow:

$$WF = WFX * W * SG60 * [1 + CEX (288.7 - TWF)] * (1/K)$$

where

SG60 fuel specific gravity at 288.7 K as determined by NASA Lewis Chemical Laboratory

CEX fuel expansion factor

TWF fuel temperature

WFX meter frequency

K meter calibration factor, a function of WFX/v

v fuel viscosity as determined from equation given in the UETP General Test Plan (ref. 4)

ω water density at 288.7 K

Calibration. - Fuel measurement system, fuel meter and appropriate length of piping, is calibrated by using a standard traceable to NBS. The method of calibration, gravimetric flow calibration, is the same as that described in detail in reference 3, Section 4.2.1.2. Calibrations were performed prior to and at the completion of each UETP entry. The calibration fluid used was water. Repeatability data were obtained at 80 percent and 10 percent of range. Typical calibration run data are shown in figure 8.

Pressure Measurement System

PSL-3 system description and calibration. - Figures 9(a) and (b) show schematics of PSL-3 pressure scanivalve system and its transducer calibration system respectively. The Scanivalve system (fig. 9(a)) consists of a Scanivalve module, which accepts 24 pressure inputs; a stepper motor to advance the Scanivalve module from port to port; a channel encoder driven in parallel with the Scanivalve module to provide output code for each of the positions (1 to 24); a strain gauge transducer; and a control box (not shown in fig. 9(a)), which housed the control electronics and the input/output interface. The valves were located outside the test cell approximately 15.24 m away from engine pressure measurement sources during the UETP tests. The system was stepped at a rate of six ports/sec. Double porting of some pressure sources measured on the same scanivalve was used to eliminate possible errors because of settling time. Each valve utilized two ports each for a low and high reference calibration pressures. Depending on pressure level, Mansfield and Green dead weight system, or a vacuum source (measured by a Digiquartz transducer) were used as sources for the calibration pressures. Each time a valve was cycled, the pressure at each port was calculated as follows:

$$Px = LRVAL + \frac{(HRVAL - LRVAL)}{(HRMV - LRMV)} * PXMV$$

where

Px unknown pressure

LRVAL low reference source pressure as determined by Digiquartz transducer

HRVAL high reference source pressure as determined by calibration weights

LRMV low reference port millivolts

HRMV high reference port millivolts

PXMV unknown pressure port millivolts

The Digiquartz transducers and the Mansfield and Green dead weight system were periodically calibrated against a standard traceable to NBS.

PSL-4 system description and calibration. - A functional diagram of the pressure system used in PSL-4 is shown in figure 10. The major components of the system are: system controller, data acquisition and control unit (DACU), pressure calibration unit (PCU), and sensor modules. The system controller interfaces the user to the DACU. Its main purpose is to program the DACU and direct data flow within the system. The DACU is a rack-mountable device which provides control and data acquisition functions for up to 512 pressure channels of sensors modules. An 8-bit microprocessor executing firmware programs controls the DACU. The DACU interfaces with the PCU and sensors through twisted pair instrumentation cables. Sensors are contained in the sensor modules and are connected to engine probes through tubing of 0.3175-cm diameter and maximum length of 15.24 m. The PCU consists of pneumatic valving and high accuracy quartz pressure transducers. The DACU, through the PCU, first pneumatically switches the sensors into the calibrate position, then applies three calibration pressures to all transducers in each pressure range. At each pressure, the electrical response of each transducer is measured. The calibration data can then be reduced by the DACU and a characteristic equation of the form shown below is generated for each transducer:

$$Px = Co + C1 * Vx + C2 * Vx^2$$

where

Co offset coefficient

C1 sensitivity coefficient

C2 nonlinearity coefficient

Vx voltage reading at Px

Px unknown pressure to be measured

Settling time between application of the calibration pressure and measurement of transducer outputs was 8 sec. Updating transducer coefficients (performing new calibration) could be done on command or automatically every 20 min. The quartz transducers were calibrated against standards traceable to NBS prior to and at the completion of each UETP entry.

Temperature Measurement System

A schematic of the temperature measurement system is shown in figure 11. Special grade type-K thermocouple wires were used in all facility and engine temperature probes. The extension wires and connectors were also made from nominal grade type-K thermocouple wires. The reference junctions were connected to ovens capable of maintaining the junction temperatures at constant level (338.7 K). The oven temperatures were recorded, using an ice point reference system, each time a scan was made. The ovens and the ice reference were periodically checked and maintained.

Speed Measurement System

Speed was measured by using tachometer generators which produce sine wave voltage output. Pulses were directly counted over a period of 1 sec with 15-bit-wide digital counters.

Area Measurement System

Diameter measurements were made with a micrometer which was accurate to 0.00254 cm (0.001 in.).

DATA ACQUISITION AND REDUCTION SYSTEMS

First Entry (PSL-3)

A schematic of the steady-state data acquisition, recording, display, and reduction system used in PSL-3 during the UETP tests is shown in figure 12. Electrical signals from all sensors were conditioned, except for temperature sensor outputs which were routed to reference ovens, prior to routing them to the data acquisition systems. Speed and fuel flow signals (sine wave) were reshaped by the frequency converter equipment to produce sharply defined square pulses which are easier to count. Pulse signals were then sent to the digital data acquisition system which consisted of several precision electronic counters. Force and pressure signals were passed through special strain-gauge signal conditioners which also supplied the required excitation voltage for the sensor's strain-gauge bridges. Temperature, pressure, and force signals were sent to the analog data acquisition system, which consisted of several amplifiers and analog to digital converters. Digital output from all channels of the data acquisition systems were then sent to the facility computer (SEL8600). The computer performed the functions of raw data recording on magnetic tape and on-line data processing and display. The magnetic tape data were sent to an IBM 3033 central computer system for batch processing. Final processed data were available on magnetic tape, microfiche, or as line printer output.

For the first entry tests, the total scanning period per reading was 20 sec. During this period, 20 scans of data from each input channel were

acquired and recorded at a rate of 1 scan/sec. Each scan of an input channel was converted to engineering units before all 20 scans were averaged to produce a single reading. During each data scan, 100 msec were used to digitize all input channels (480 channels). Table I presents a complete data acquisition time summary describing all functions performed during a scan.

With the exception of pressure sensors, all other instruments remained at their respective positions (sensors were not exercized between load and 29-load positions each time a scan was taken) during the total scanning period resulting in only one instrument dwell per reading. Because of the calibration method used for the Scanivalve pressure system, its sensors were exercized five times during the total scanning period. The number of instrument dwells affects the instrument precision error by reducing it by an amount proportional to the reciprocal of the square root of the number of dwells. This number is different from the number of scans per reading. Scans were obtained at a constant instrument position.

Second Entry (PSL-4)

A schematic of the steady-state data acquisition, recording, display, and reduction system used during UETP second entry tests is shown in figure 13. The equipment used to condition and route the speed, fuel flow, temperature, and force signals to the data acquisition systems were the same as in PSL-3. The pressure measurement system was changed to an electronic scanning pressure system as described in the previous section. Raw data from the digital and analog data acquisition systems and engineering units data (pressure) from the electronic scanning pressure system were transferred through the PDP11 computer (located in the test facility) to the VAX computer (located in the central computer building). The VAX computer provided on-line conversion to engineering units, calculation of performance parameters, and transfer of processed data back to the PDP11 computer for limit checking and CRT displays at the facility. The VAX computer also transferred engineering units data to a central computer for final data reduction and analysis.

During the second entry tests, the total scanning period per reading was 30 sec. During this period, 20 scans of data from each input channel were acquired and recorded at a rate of one scan per 1.5 sec. One scan from each channel consists of one frame of data except for pressure channels where one scan consists of the average of four frames obtained at a rate of one frame every 0.024 sec. Each channel's 20 scans were first converted to engineering units and then averaged to produce a single value for the reading. Two hundred-fifteen milliseconds were used to acquire all the data (480 channels) during each scan. Table II presents a complete data acquisition time summary describing all functions performed during a scan. In terms of instrument dwells, all sensors remained at their respective positions during the total scanning period resulting in one dwell per reading.

A summary of the pertinent data acquisition parameters is given in table III. Table III lists, for each measured variable, the total number of probes, the total scanning period, the number of scans per reading, and the number of instrument dwells per reading.

MEASUREMENT UNCERTAINTY METHODOLOGY

The process used in this report for determining measured performance parameter errors is based on the method specified in the UETP General Test Plan (ref. 4) and follows the approach of reference 3. The method involves the following steps:

(1) Determination of all elemental errors, both biases and precisions, for each measured variable involved in a performance parameter calculations. These errors will be referred to hereafter as:

b_{ij} = i^{th} elemental bias error for the j^{th} measured variable in percent of reading

s_{ij} = i^{th} elemental precision error for the j^{th} measured variable in percent of reading

(2) Determination of total bias and precision errors for each measured variable as follows:

$$B_j = \sqrt{\sum_i (b_{ij})^2}$$

$$S_j = \sqrt{\sum_i (s_{ij})^2}$$

where

B_j total bias for the j^{th} measured variable in percent of reading

S_j total precision for the j^{th} measured variable in percent of reading

(3) Determination of total uncertainty for each measured variable in percent of reading

$$U_j = \pm (B_j + t95 * S_j)$$

where

U_j total uncertainty for the jth measured variable in percent of reading

t95 ninety-fifth percentile point for the two-tailed Student "t" distribution and is a function of the degrees of freedom used to calculate S_j. A value of 2.0 was chosen in this report.

(4) Determination of each performance parameter influence coefficients. These coefficients, defined in reference 3 as the partial derivatives of the performance parameter with respect to each measured variable, were estimated in this report by calculating the percent change in a performance parameter (ΔG) because of a 1 percent change in a measured variable (ΔX). This was done

by perturbing by 1 percent each measured variables in the UETP data reduction program. These coefficients will be referred to hereinafter as $\Delta G/\Delta X$.

(5) The final step is the propagation of the measured variable errors to each performance parameter by using the Taylor's series formula (ref. 3)

$$B_G = \sqrt{\left(\frac{\Delta G}{\Delta X_1} * B_1\right)^2 + \ldots + \left(\frac{\Delta G}{\Delta X_j} * B_j\right)^2}$$

$$S_G = \sqrt{\left(\frac{\Delta G}{\Delta X_1} * S_1\right)^2 + \ldots + \left(\frac{\Delta G}{\Delta X_j} * S_j\right)^2}$$

The total uncertainty is then calculated as

$$U_G = B_G + 2 * S_G$$

where

B_G performance parameter bias error, percent of reading

S_G performance parameter precision error, percent of reading

U_G performance parameter uncertainty, percent of reading

$\frac{\Delta G}{\Delta X_j}$ change in the performance parameter (G) due to 1 percent change in the j^{th} measured variable (X_j)

B_j total bias error of the j^{th} measured variable

S_j total precision of the j^{th} measured variable

RESULTS AND DISCUSSION

An error analysis was conducted to determine the bias, precision, and uncertainty of measured J57 turbojet engine performance parameters. With the same engine, performance parameters were measured twice, once, during tests conducted in test cell number 3 and again during tests conducted in test cell number 4 of the NASA Propulsion Systems Laboratory. The tests were conducted as a part of the UETP program which was sponsored by AGARD. The analysis covered 15 performance parameters measured at a high rotor speed of 8875 rpm at three engine flight conditions referred to as test condition 3 (P2 = 82.7 kPa, T2 = 288 K, P2/PAMB = 1.0), test condition 6 (P2 = 82.7 kPa, T2 = 288 K, P2/PAMB = 1.3), and test condition 9 (P2 = 20.7 kPa, T2 = 288 K, P2/PAMB = 1.3). The results are discussed in terms of the measured variable errors in appendix A and table IV, the performance parameter influence coefficients as presented in table V, and the performance parameter errors (bias, precision, and uncertainty) as presented in table VI.

Appendix B presents an error audit for variables as they were measured in PSL4. A similar audit was performed for the same measured variables during tests in PSL3. The audit was initiated and developed by AEDC and was finalized by the North American participants in the UETP program (NRC, AEDC, NASA,

NAPC). It consists of three parts for each of the six measurement systems (force, fuel flow, pressure, temperature, speed, and area). The first part is an elemental error source description. The second is the error source evaluation which lists elemental error source (b_i and s_i), test condition (numbers 3, 6, and 9), the absolute value of the magnitude of the error for each measured variable, and comments about the method used to determine the error. Also included as part of the evaluation is a list of measured variables total bias, precision, and uncertainty, calculated as described in the previous section. The third part is an elemental error source diagram (figs. B-1 to B-6). In general, the data in this appendix indicate no consistency in the type of major contributors to the total bias between the six measurements. For example, the magnitudes of the force measurement system elemental biases, in descending order, are as follows: b20 (calibration data curve fit), b1 (standard laboratory calibration), and b19 (channel measurement error). However, the magnitudes for the temperature measurement system, in descending order, are as follows: b1 (standard laboratory calibration), b2 (reference system), and b7 (measurement channel). In terms of the elemental precision errors, no one source is dominant since actual post test data were used to calculate the precision resulting from a combination of sources.

Table IV summarizes the results of the error evaluation for all required variables as they were measured in PSL-3 and PSL-4. The table consists of two main columns: measured variables and errors. The first column lists the name of each measured variable and its nominal value, as measured in PSL-3 and PSL-4 for each test condition at a high rotor speed of 8875 rpm. The second column lists, for PSL-3 and PSL4, total bias, total precision, and total uncertainty for each measured variable at each test condition. There were 22 measured variables if the fuel lower-heating value (LHV) is included. A fuel analysis done at NASA Lewis supplied one value for the LHV error. Precision and bias were calculated by using the assumption of uniform error distribution as described in reference 3.

The errors listed in table IV are the same as those listed in appendix B, (PSL-4) except that here they are given in percent of reading. Also, the precision errors were reduced, from those shown in appendix B, by the reciprocal of the square root of the number of probes used to average each measured variable. However, the number of scans per reading (20) was not used in a similar fashion, since the majority of the instrument systems were not exercised each time a scan was taken (i.e., only one dwell per reading). In general, the data in this table show that (1) measured variable error levels in PSL-3 and PSL-4 were comparable (except for PS7 and P7), (2) error levels increased significantly for test condition 9 (low pressure levels) because of the assumption of constant absolute levels of elemental errors over the complete range of a measurement system, and (3) bias errors are two to three times higher than precision errors.

The influence of the measured variables on each performance parameter is given in terms of the influence coefficients presented in table V. The table consists of two main columns, measured variables, and performance parameter influence coefficients. The first column lists the name of the measured variables, the test cell, and the test conditions. The second column lists the influence coefficients ($\Delta G/\Delta X$) for the 15 performance parameters. It is apparent from this table that level and sign of these coefficients, for any performance parameter, were comparable between test cell numbers 3 and 4.

However, for FN, SFC, FNRD, and SFCRD, both the level and sign changed from condition 3 to condition 6 or 9, regardless of test cell, for some measured variables. For example, for PSL-3, the influence coefficient of the performance parameter FN, because of the measured variable P1, went from +2.086 percent for condition number 3 to +0.834 and +0.805 percent for condition numbers 6 and 9, respectively. Also, the coefficients of PS1 for SFC went from 0.703 percent for condition number 3 to -0.396 and -0.465 percent for condition numbers 6 and 9, respectively. The reason for these changes is due to the change in engine ram ratio from 1.0 for condition number 3 to 1.3 for condition numbers 6 and 9, thereby resulting in different changes in the FN term of WA1 * Vo (ram term).

The most valuable information that can be extracted from this table is the sorting out of the measured variables of a performance parameter in terms of the magnitude of their influence on the parameter. For example, the measured variables which caused the most influence on FN for PSL-3, condition number 3 are, in descending order: P2 (4.724), PAMB (2.77), P1 (2.086), FS (0.915), PS1 (0.697), PBOAT (0.613), A1 (0.099), PSEAL (0.036), TAIR (0.031), T2 (0.027), ASEAL (0.013), TM1 (0.002).

Following the methodology described in the previous section, measured variable errors were propagated to the performance parameters through the influence coefficients with the results given in table VI. This table consists of two main columns: performance parameter and errors. The first lists the name of the performance parameter, the test cell, and the test conditions, the second lists, in percent of the nominal value of the performance parameter, the total bias, the total precision, and the total uncertainty. The data in this table show the following:

(1) For most performance parameters at a given test condition, error levels, bias, precision, and uncertainty, were comparable between measurements made in test cell numbers 3 and 4.

(2) For any performance parameter at either test cell, error levels increased significantly as test conditions were changed from numbers 3 or 6 to 9 because of a decrease in pressure levels.

(3) For any performance parameter, the total bias error was two to three times higher than total precision error.

(4) There were insignificant differences in errors between corrected and uncorrected airflow, net thrust, and specific fuel consumption.

CONCLUSIONS

As a requirement of the UETP, NASA Lewis performed an uncertainty analysis of engine performance parameters as measured in the Lewis Propulsion Systems Laboratory. A summary of the results of that analysis is as follows:

1. As a result of the UETP, a measurement uncertainty methodology was developed which makes the NASA Lewis results comparable to those generated by the other facilities which participated in the UETP.

2. Most engine performance parameter measurements in the NASA Lewis Propulsion Systems Laboratory test cell numbers 3 and 4 had the same error levels in terms of bias, precision, and uncertainty.

3. As a percent of reading, performance parameter error levels increased with decreasing pressure.

4. Performance parameter bias error levels were two to three times higher than those of precision errors.

5. For net thrust, the measured variables having the greatest influence, in descending order, are as follows: P2, PAMP, P1, FS, PS1, PBOAT, A1, PSEAL, TAIR, T2, ASEAL, and TM1.

6. There were insignificant differences in error between corrected and uncorrected airflow, net thrust, and specific fuel consumption.

APPENDIX A - SYMBOLS

ABOAT	exhaust nozzle boattail area, (A7 - A8), m^2
AS	area at inlet duct Labyrinth seal, m^2
ASEAL	labyrinth seal area, (AS - A1), m^2
AWET	wetted area between plane at start of inlet ducting and plane at airflow measuring station, π * D1 * L1, m^2
A1	area at engine inlet airflow measurement plane, m^2
A7	area at exhaust nozzle inlet plane, m^2
A8	area at exhaust nozzle exit plane, m^2
B_G	the G performance parameter total bias, percent
B_j	total bias for the j^{th} measured variable, percent
bij	ith elemental bias error for the j^{th} measured variable, percent
CEX	fuel expansion factor
CD8	station 8 (plane of engine exhaust nozzle exit) flow coefficient based on facility airflow rate measurement
CF	flat plate drag coefficient at zero angle of attack
CG8	exhaust nozzle thrust coefficient
Co	offset coefficient
CV8	exhaust nozzle velocity coefficient
C1	sensitivity coefficient
C2	nonlinearity coefficient
D1	diameter at station 1 airflow measuring station, m
FBOAT	pressure force on exhaust nozzle boattail, ABOAT * (PBOAT - PAMB), N
FD	force caused by flow on the inside diameter between labyrinth seal inlet plane and facility airflow measurement plane, GAM1 * CF * PS1 * M1 * AWET, N
FDAP	calibrated force caused by flow through the labyrinth seal and the test cell, N

FG	engine gross thrust, N
FM	facility thrust bed force measurement, N
FN	engine net thrust, N
FNRD	engine net thrust referred to desired conditions, N
FP	facility thrust bed preload force measurement, N
FS	facility thrust bed scale force measurement, FM - FP + FTARE + FDAP + FD, N
FSEAL	pressure force on labyrinth seal area, ASEAL * (PSEAL - PAMB), N
FTARE	calibrated force caused by thrust stand support and service system, N
F1	engine inlet total momentum, WA1 * V1 + A1 (PS1 - PAMB), N
G	general notation for performance parameters
GAM1	specific heat at station 1
GPM	gallons per minute
HRMV	mechanical scanivalve system high reference pressure port millivolt output
HRVAL	mechanical scanivalve system high reference port pressure, kPa
K	fuel meter calibration factor, cycles/gal
LHV	fuel lower heating value, J/N
LRMV	mechanical scanivalve system low reference pressure port millivolt output
LRVAL	mechanical scanivalve system low reference pressure port pressure, kPa
L1	length between inlet of labyrinth seal and facility airflow measuring planes, m
NH	high-pressure compressor speed, rpm
NHRD	high-pressure compressor speed referred to desired conditions, rpm
NL	low-pressure compressor speed, rpm
NLRD	low-pressure compressor speed referred to desired conditions, rpm
PAMB	ambient pressure, kPa
PBOAT	average static pressure at station 0.4, kPa

PS1	average static pressure at station 1, kPa
PS7	average static pressure at station 7, kPa
PS7Q2	PS7/P2
PSEAL	average static pressure at station 0.1, 0.2, kPa
Px	unknown pressure to be measured by pressure measurement system
(Px)mv	unknown pressure port millivolt output
P1	average total pressure at facility airflow measuring plane, kPa
P2	average total pressure at station 2, kPa
P7	average total pressure at station 7, kPa
P7Q2	P7/P2
SFC	engine specific fuel consumption, g/N s
SFCD	SFC referred to desired conditions, g/N s
SF60	fuel specific gravity at 288.7 K
S_G	the G performance parameter total precision, percent
S_j	total precision for the j^{th} measured variable, percent
S_{ij}	jth elemental precision error for the j^{th} measured variable, percent
TAIR	average total temperature at station 0, K
TM1	average metal temperature at station 1, K
TM7	average metal temperature at station 7, K
TWF	average fuel temperature, K
T2	average total temperature at station 2, K
T7	average total temperature at station 7, K
T7Q2	T7/T2
t95	95th percentile point for the two-tailed student "t" distribution
U_G	the G performance parameter total uncertainty, percent
U_j	uncertainty for the jth measured variable, percent
Vo	free stream velocity, m/sec

Vx	voltage at Px
V1	velocity at station 1, m/sec
W	water density, g/gal
WA1	airflow rate at station 1, kg/s
WA1RD	airflow rate referred to desired conditions, kg/s
WF	engine fuel flow rate, g/s
WFRD	engine fuel flow rate referred to desired conditions, g/s
WFX	fuel flow, meter output, Hz
X	a random measured variable
Δ	change in parameter

APPENDIX B - PSL-4 ERROR AUDIT

Elemental Error Source Description for Force Measurement System

Error	Type	Error Description
b_1	s_1	Error from standard lab calibration of load cells, including traceability to national standards
b_2	s_2	Error due to misalignment between the engine force vector and the force vector measured by the data load cell train
b_3	s_3	Error due to shift in load cell calibration caused by attachement of adaptors and flexures
b_4	s_4	Error due to pressurization of the labyrinth seal
b_5	s_5	Error caused by the measurement of the forces on an axis different from the engine centerline
b_6	s_6	Error due to the system hysteresis
b_7	s_7	Error due to the system nonrepeatability, as determined by repeated calibration both pre- and post-test
b_8	s_8	Error due to the system nonlinearity
b_9	s_9	Error due to the effect of changes in cell pressure on the load cell
b_{10}	s_{10}	Error due to the effect of changes in cell pressure on the test cell wall which is the thrust system ground
b_{11}	s_{11}	Error due to the effect of changes in line pressure on the tare forces exerted on the thrust measurement system by propellant lines, etc., routed to the engine
b_{12}	s_{12}	Error due to the effect of a change in temperature on the load cell
b_{13}	s_{13}	Error due to the effect of changes in temperature on the tare forces exerted on the thrust measurement system by lines routed to the engine
b_{14}	s_{14}	Error due to thermal growth of the thrust stand
b_{15}	s_{15}	Error due to inlet air ram effects on sea level test stands
b_{16}	s_{16}	Error due to secondary airflow external drag effects on engine surface and service lines

Error	Type	Error Description
b_{17}	s_{17}	Error due to the effect of vibration on the load cell
b_{18}	s_{18}	Error due to the effect of vibration on the thrust stand
b_{19}	s_{19}	Error from signal conditioning, shunt calibration, and digital system
b_{20}	s_{20}	Error from curve fit of calibration data
b_{21}	s_{21}	Error associated with the ability to determine a time interval when the data varies due to plant or engine instability

TABLE B-I. - ELEMENTAL ERROR SOURCE EVALUATION FOR FORCE MEASUREMENT SYSTEM

[Measured variables, scale force (FS); range, condition 3, 6, 9 at NH = 8875 rpm.]

(a) Elemental errors

Source	Magnitude, N (lbf)			Comments
	Condition 3	Condition 6	Condition 9	
b1 s1	±22.7(5.1) ±8.0(1.8)	±22.7(5.1) ±8.0(1.8)	±22.7(5.1) ±8.0(1.8)	Estimated from traceability information and standard laboratory calibration data
b2 s2	(a)	(a)	(a)	Negligible error; based on engineering estimate that alignment between engine center line and load cell measurement centerline is accurate
b3 s3	(a)	(a)	(a)	Estimated based on load cell calibration repeatability including pre- and post-test calibration; included in s19
b4 s4	0(0) ±25.8(5.8)	0(0) ±27.6(6.2)	0(0) ±17.8(4)	Estimated from test facility flow calibration data, these data are obtained to determine forces caused by flow through the labyrinth seal and test cell (cooling air). Calibration test consists of blanking off the inlet duct downstream of the labyrinth seal, flowing air through the seal and the test cell, and measuring the resultant forces. Data are obtained at inlet and cell pressures corresponding to each test condition.
b5 s5	(a)	(a)	(a)	Negligible error; design considerations of thrust bed and support system reduce error to negligible magnitude
b6 s6	0(0) ±13.3(3)	0(0) ±13.3(3)	0(0) ±13.3(3)	Estimated from test stand force calibration data which are obtained to determine forces caused by thrust stand support and service systems. Calibration tests are conducted before engine starts and after engine shutdowns at sea level and altitude conditions; thus making this error a combined value, accounting for error source 6, 7, 8, 10, 11, 13, and 14.
b9 s9	0(0) ±8.9(2)	0(0) ±8.9(2)	0(0) ±8.9(2)	Estimated from electrical calibration data obtained to determine environmental effects on load cells, which are vented to cell pressure and water cooled. Calibration data are obtained before engine starts and after engine shutdowns at sea level and altitude conditions; thus making this error a combined value accounting for error source 9 and 12.

[a]Magnitude = 0 N (lbf).

TABLE B-I. - Continued.

Source	Magnitude, N (lbf)			Comments
	Condition 3	Condition 6	Condition 9	
b15 s15	(a)	(a)	(a)	Not applicable
b16 s16	(a)	(a)	(a)	Included in s4
b17 s17	(a)	(a)	(a)	Negligible error; 1 Hz filters installed in load cell measurements channels.
b18 s18	(a)	(a)	(a)	Negligible error
b19 s19	±17.8(4) 24.9(5.6)	±17.8(4) ±24.9(5.6)	±17.8(4) 24.9(5.6)	Estimated from data system specifications and NASA Lewis UETP data by using the method described in reference 3, appendix C
b20 s20	±62.3(14.0) 0(0)	±62.3(14.0) 0(0)	±62.3(14.0) 0(0)	Estimated as the root-sum-square of differences between curve fit and calibration data
b21 s21	(a) (a)	(a) (a)	(a) (a)	Negligible error; 1 Hz filters and data averaging reduce error to negligible magnitude. Each data point consists of the average of 20 samples taken at a rate of one sample every 1.5 sec.

(b) Total errors[b]

Condition	Error, N (lbf)		
	Total system bias, B	Total system precision, S	Total system uncertainty, U
3	68.6(15.4)	40.1(9.0)	148.8(33.4)
6	68.6(15.4)	41.3(9.3)	151.2(34.0)
9	68.6(15.4)	35.5(8.0)	139.6(31.4)

[a]Magnitude = 0 N (lbm).

[b]Total system bias, $B = \sqrt{(b1)^2 + (b19)^2 + (b20)^2}$; total system precision,

$S = \sqrt{(s1)^2 + (s4)^2 + (s6)^2 + (s9)2 + (s19)2}$; total system uncertainty, $U = \pm (B + 2 * S)$.

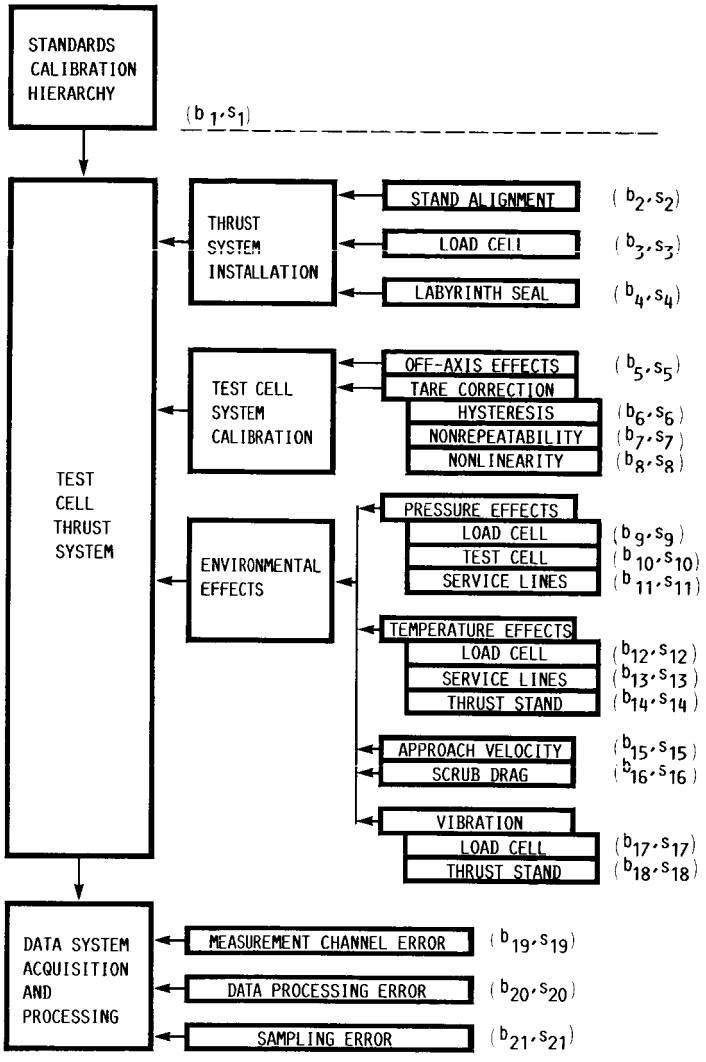

FIGURE B-1.- ELEMENTAL ERROR SOURCE DIAGRAM FOR FORCE MEASUREMENT SYSTEM.

Elemental Error Source Description for Fuel Flow Measurement System

Error	Type	Error Description
b_1	s_1	Error from standard lab calibration of flowmeter, including traceability to national standards
b_2	s_2	Error due to the effect of cavitation caused by insufficient static pressure within the flowmeter
b_3	s_3	Error due to the effect of turbulent flow caused by sharp bends, etc. upstream of the flowmeters
b_4	s_4	Error due to the effect of orientation differences from calibration to application
b_5	s_5	Error from determination of calibration fluid specific gravity, viscosity, and matching these to the characteristics of the test fluid to be used
b_6	s_6	Error due to the flowmeter nonrepeatability from repeat flowmeter calibration, including difference between pre- and post-test calibrations
b_7	s_7	Error from the effect of ambient temperature changes on the flowmeter
b_8	s_8	Error in the determination of test fluid viscosity
b_9	s_9	Error in the determination of test fluid specific gravity
b_{10}	s_{10}	Error from the effect of vibration on the flowmeter
b_{11}	s_{11}	Error from the effect of ambient pressure changes on the flowmeter
b_{12}	s_{12}	Error associated with the ability to determine a representative value over a specified time interval when the data are varing due to fuel pressure or engine instability
b_{13}	s_{13}	Error from signal conditioning calibration oscillator and digital system
b_{14}	s_{14}	Error from curve fits of calibration data and fluid property correction

TABLE B-II. - ELEMENTAL ERROR SOURCE EVALUATION FOR FUEL FLOW MEASUREMENT SYSTEM

[Measured variables, facility fuel flow (WF); range, condition 3, 6, 9 at NH = 8875 rpm.]

(a) Elemental errors

Source	Magnitude, g/s (lbm/hr)			Comments
	Condition 3	Condition 6	Condition 9	
b1 s1	0.55(4.4) .10(.80)	0.55(4.4) .10(.80)	0.16(1.3) .02(.20)	Estimated from calibration traceability information
b2 s2	(a)	(a)	(a)	Negligible error; fuel pressure is kept high enough to prevent cavitation
b3 s3	(a)	(a)	(a)	Negiligible error; fuel flow measurement pipe upstream and dowstream straight sections are greater than 20 diameters in length
b4 s4	(a)	(a)	(a)	Negligible error; fuel flow measurement pipe calibration and installation orientations are the same
b5 s5	(a)	(a)	(a)	Negligible error; water is used as calibration fluid. Corrected frequency (f/v) is used to determine K-factor
b6 s6	(a)	(a)	(a)	Shift in meter K-factor between pre- and post-calibration included in s13
b7 s7	.83(6.6) 0(0)	.25(2.0) 0(0)	.50(4.0) 0(0)	Estimated by using ISA procedure for calculating error introduced by dimensional changes due to differences in operating and calibration temperatures
b8 s8	(a)	(a)	(a)	Nigligible error; viscosity determination method is the same for all test facilities
b9 s9	.94(7.5) 0(0)	.94(7.5) 0(0)	.28(2.2) 0(0)	Based on NASA Lewis chemical lab estimate of specific gravity error and estimate of fuel temperature error
b10 s10	(a)	(a)	(a)	Negligible error
b11 s11	(a)	(a)	(a)	Negligible error
b12 s12	(a)	(a)	(a)	Negligible error; data averaging reduce error to negligible magnitude. Each data point consists of the average of 20 samples taken at a rate of one sample every 1.5 sec.
b13 s13	.50(4.7) 1.57(12.50)	.50(4) 1.57(12.5)	.13(1) .79(6.30)	Estimated from channel specifications data and NASA Lewis UEIP data by using the method described in reference 3, appendix C
b14 s14	2.78(22.1) 0(0)	2.78(22.1) 0(0)	.83(6.60) 0(0)	Estimated as maximum difference between curve fit and calibration data

(b) Total errors[b]

Condition	Error, g/s (lbm/hr)		
	Total system bias, B	Total system precision, S	Total system uncertainty, U
3	3.1(25.1)	1.6(12.5)	6.3(50.1)
6	3.0(24.2)	1.6(12.5)	6.2(49.2)
9	1.0(8.2)	.8(6.3)	2.6(20.8)

[a]Magnitude = 0 g/s (lbm/hr).

[b]Total system bias, $B = \sqrt{(b1)^2 + (b7)^2 + (b9)^2 + (b13)^2 + (b14)^2}$; total system precision, $S = \sqrt{(s1)^2 + (s13)^2}$; total system uncertainty, $U = \pm (B + 2 * S)$.

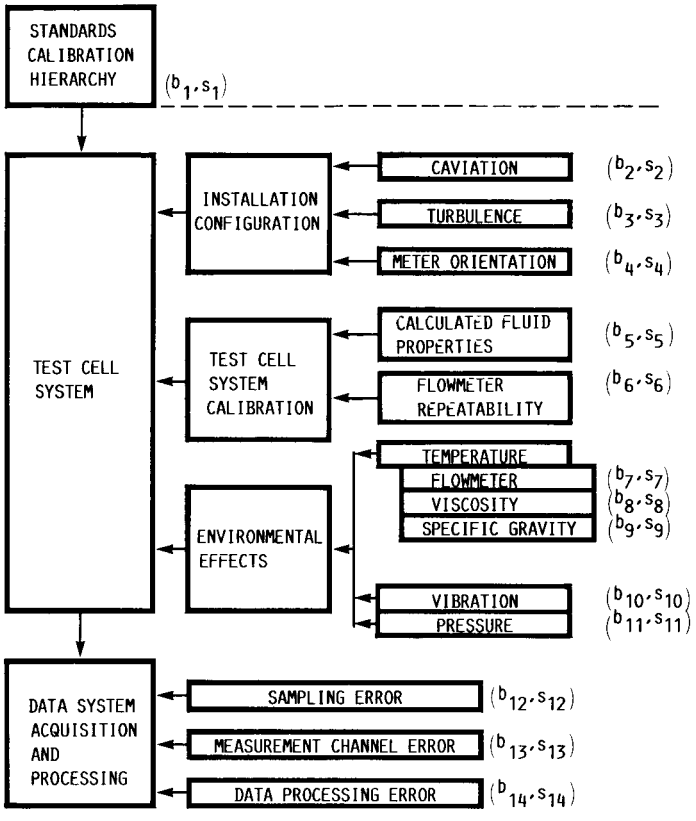

FIGURE B-2. - ELEMENTAL ERROR SOURCE DIAGRAM FOR FUEL FLOW MEASUREMENT SYSTEM.

Elemental Error Source Description for Fuel Flow Measurement System

Error	Type	Error Description
b_1	s_1	Error from the standards lab calibration of the in place pressure generator or the sensor calibration, including traceability to national standards
b_2	s_2	Error from the design and fabrication of the static or total pressure probe
b_3	s_3	Error from the design and fabrication of the reference pressure probe for delta pressure measurements
b_4	s_4	Error due to changes in transducer calibration with line pressure for delta pressure sensors
b_5	s_5	Error from the determination of reference pressure
b_6	s_6	Error due to sensor hysteresis
b_7	s_7	Error due to sensor nonlinearity
b_8	s_8	Error due to sensor nonrepeatability
b_9	s_9	Error due to the effect of changes in temperature on the pressure sensor
b_{10}	s_{10}	Error due to the effect of vibration on the pressure sensor
b_{11}	s_{11}	Error due to the effect of changes in line pressure on delta pressure sensors
b_{12}	s_{12}	Error associated with the ability to determine a representative value over a specified time interval when the data are varing due to plant or engine instability
b_{13}	s_{13}	Error from signal conditioning, electrical calibration, and digital system
b_{14}	s_{14}	Error from curve fit of calibration data

TABLE B-III. - ELEMENTAL ERROR SOURCE EVALUATION FOR PRESSURE MEASUREMENT SYSTEM

[Measured variables, P1, PS1, P2, P7, PS7, PAMB, PBOAT, PSEAL; range, condition 3, 6, 9 at NH = 8875 rpm.]

Source	Condition	Magnitude, kPa (psi)				Comments
		P1, PS1	P2	P7, PS7	PAMB, PBOAT, PSEAL	
b1 s1	3, 6, 9 3, 6, 9	0(0) .034(.005)	0(0) .034(.005)	0(0) .172(.025)	0(0) .034(.005)	Estimated from specifications data for the calibration pressure measurement system
b2 s2 b2 s2 b2 s2	3 6 9 	.055(.008) 0(0) .076(.011) 0(0) .021(.003) 0(0)	(a)	(a)	(a)	This error applies only to static pressure measurement and is due to wall static pressure hole size. Design considerations reduce total pressure probe errors to negligible magnitude.
b3 s3	3, 6, 9	(a)	(a)	(a)	(a)	Not applicable to NASA Lewis
b4 s4	3, 6, 9	(a)	(a)	(a)	(a)	Negligible error; system calibrated every 20 min by using three-point calibration pressures covering the range of test pressures
b5 s5	3, 6, 9	(a)	(a)	(a)	(a)	Negligible error
b6 s6	3, 6, 9	.055(.008) .028(.004)	.055(.008) .028(.004)	.524(.076) .083(.012)	.055(.008) .028(.004)	Estimated from system's specifications data and NASA Lewis UETP data with the method described in AEDC-TR-73-5, section 5.2.2. This is a combined value accounting for error source 6, 7, 8, 13, and 14.
b9 s9	3, 6, 9	(a)	(a)	(a)	(a)	Negligible error; on-line system calibration removes environmental error. This is a combined value accounting for error source 9, 10, and 11.
b12 s12	3, 6, 9	(a)	(a)	(a)	(a)	Negligible error; data averaging reduce error to negligible magnitude. Each data point consists of the average of 20 samples taken at a rate of one sample every 1.5 sec.

[a]Magnitude = 0 kPa (psi).

TABLE B-III. - Concluded.

(b) Total errors[b]

Error	Condition	Magnitude, kPa (psi)					
		P1	PS1	P2	P7	PS7	PAMB, PBOAT, PSEAL
Bias, B	3	0.055(.008)	0.078(.011)	0.055(.008)	0.524(.076)	0.524(.076)	0.055(.008)
	6	.055(.008)	.094(.014)	.055(.008)	.524(.076)	.524(.076)	.055(.008)
	9	.055(.008)	.059(.009)	.055(.008)	.524(.076)	.524(.076)	.055(.008)
Precision, S	3	.044(.006)	.044(.006)	.044(.006)	.191(.028)	.191(.028)	.044(.006)
	6	.044(.006)	.044(.006)	.044(.006)	.191(.028)	.191(.028)	.044(.006)
	9	.044(.006)	.044(.006)	.044(.006)	.191(.028)	.191(.028)	.044(.006)
Uncertainty, U	3	.143(.021)	.166(.024)	.143(.021)	.906(.131)	.906(.131)	.143(.021)
	6	.143(.021)	.182(.026)	.143(.021)	.906(.131)	.906(.131)	.143(.021)
	9	.143(.021)	.147(.022)	.143(.021)	.906(.131)	.906(.131)	.143(.021)

[b]Total system bias, $B = \sqrt{(b2)^2 + (b6)^2}$; total system precision, $S = \sqrt{(s1)^2 + (s6)^2}$; total system uncertainty, $U = \pm(B + 2 * S)$.

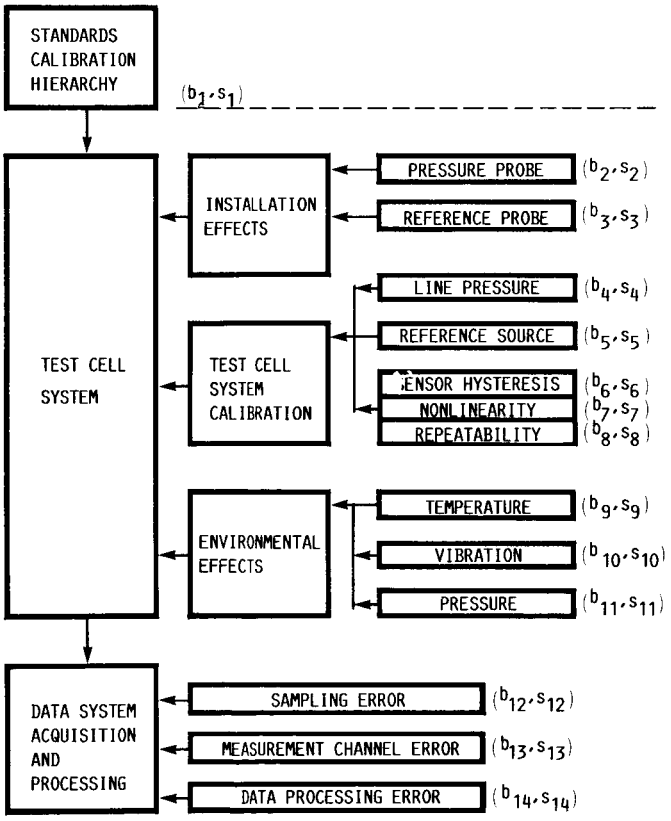

FIGURE B-3.- ELEMENTAL ERROR SOURCE DIAGRAM FOR PRESSURE MEASUREMENT SYSTEM.

Elemental Error Source Description for Temperature Measurement System

Error	Type	Error Description
b_1	s_1	Error due to manufacturer specification of wire or standard lab calibration, which ever is used
b_2	s_2	Error due to reference temperature level
b_3	s_3	Error due to reference temperature stability
b_4	s_4	Error due to probe design caused by radiation, friction, etc., when measuring gas temperatures
b_5	s_5	Error due to heat conduction
b_6	s_6	Error due to temperature gradients along nonhomogenious thermocouple wire
b_7	s_7	Error from signal conditioning, millivolt calibration source, and digital system
b_8	s_8	Error from curve fit of thermocouple tables furnished by national standards laboratory
b_9	s_9	Error associated with the ability to determine a representative value over a specified time interval when the data are varing because of plant or engine instability

TABLE B-IV. - ELEMENTAL ERROR SOURCE EVALUATION FOR TEMPERATURE MEASUREMENT SYSTEM

[Measured variables, TAIR, T2, T7, TM1, TM7; range, condition 3, 6, 9 at NH = 8875 rpm.]

(a) Elemental errors

Source	Magnitude, K (°F)			Comments
	TAIR	T2	T7	
b1 s1	1.11(2.0) 0(0)	1.11(2.0) 0(0)	2.17(3.9) 0(0)	Manufacturer's limit of error on special grade K-type thermocouple wire
b2 s2	0.41(.74) 0(0)	0.41(.74) 0(0)	0.41(.74) 0(0)	Estimated from specifications data of reference ovens
b3 s3	0(0) 0.28(.5)	0(0) 0.28(.5)	0(0) 0.28(.5)	Estimated from specifications data of reference ovens
b4 s4	(a)	(a)	(a)	Recovery correction as estimated from NASA TP1099
b5 s5	(a)	(a)	(a)	Negligible error; probe design considerations reduce error to negligible magnitude
b6 s6	(a)	(a)	(a)	Negligible error; small gradients
b7 s7	.28(.5) .11(.2)	.28(.5) .11(.2)	.28(.5) .11(.2)	Estimated by using method specified in ref. 3, section 5.3.2.1; this is a combined value accounting for error 7 and 8.
b9 s9	(a)	(a)	(a)	Negligible error; data averaging reduce error to negligible magnitude. Each data point consists of the average of 20 samples taken at a rate of one sample every 1.5 sec.

(b) Total errors[b]

Parameter	Error, K (°F)		
	Total system bias, B	Total system precision, S	Total system uncertainty, U
TAIR	1.2(2.2)	.30(.54)	1.8(3.3)
T2	1.2(2.2)	.30(.54)	1.8(3.3)
T7	2.2(4.0)	.30(.54)	2.8(5.1)
TM1	1.2(2.2)	.30(.54)	1.8(3.3)
TM7	2.2(4.0)	.30(.54)	2.8(5.1)

[a]Magnitude = 0 K (°F).

[b]Total system bias, $B = \sqrt{(b1)^2 + (b2)^2 + (b7)^2}$; total system precision $S = \sqrt{(s3)^2 + (s7)^2}$;

total system uncertainty, $U = \pm(B + 2 * S)$.

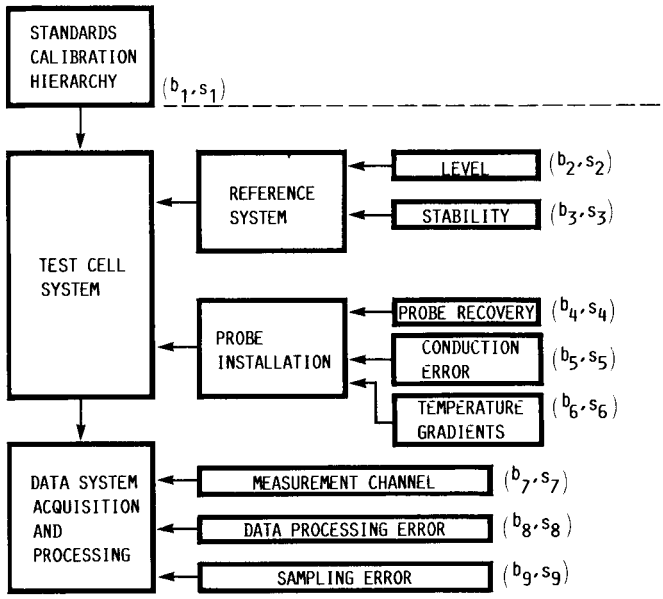

FIGURE B-4. - ELEMENTAL ERROR SOURCE DIAGRAM FOR TEMPERATURE MEASUREMENT SYSTEM.

Elemental Error Source Description for Rotor Speed Measurement System

Error	Type	Error Description
b1	s1	Standards lab calibration of frequency calibration source, including traceability to national standards
b2	s2	Error from sensor design (gear-tooth shape, etc.)
b3	s3	Error from rotor mount (gear ratio)
b4	s4	Error due to the effect of vibrations on the speed sensor
b5	s5	Error from signal conditioning, calibration oscillator, and digital system
b6	s6	Error from calibration curve fit
b7	s7	Error associated with the ability to determine a representative value over a specified time interval when the data are varing because of engine instability

TABLE B-V. - ELEMENTAL ERROR SOURCE EVALUATION FOR ROTOR SPEED MEASUREMENT SYSTEM

[Measured variables, NH, NL; range, 8875 rpm for NH, 5300 rpm for NL; total system bias, B = 1.2 rpm for NH, (0.8 rpm for NL); total system precision, S = 0 rpm for NH and NL; total system uncertainty, U = B + 2 * S = 1.2 rpm for NH, (0.8 rpm for NL).]

Source	Magnitude, rpm	Comments
b1 s1	0	Internal data system oscillator used to periodically check counter
b2 s2	0	Negligible error
b3 s3	0	Negligible error
b4 s4	0	Negligible error
b5 s5	1.2 0	Estimated from data system specifications; this is a combined value accounting for error source 5, 6, and 7. A value of 0.8 rpm was estimated for NL.

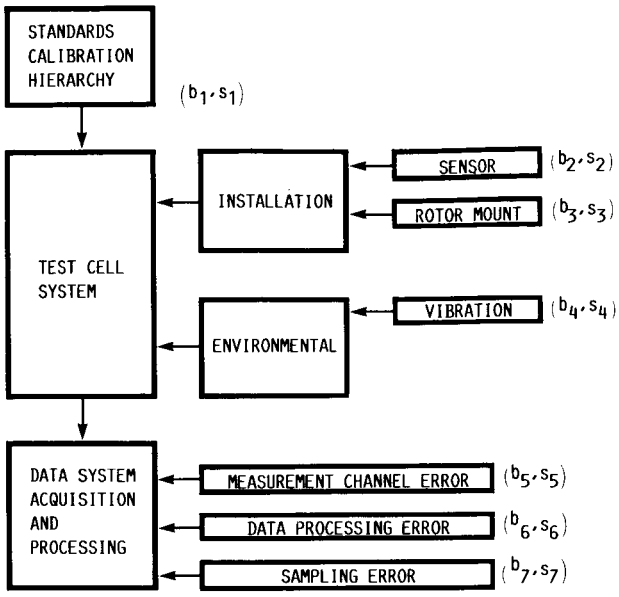

FIGURE B-5. - ELEMENTAL ERROR SOURCE DIAGRAM FOR ROTOR SPEED MEASUREMENT SYSTEM.

Elemental Error Source Description for Area Measurement System

Error	Type	Error Description
b_1	s_1	Error from the standards laboratory calibration of the precision instrument used to make the physical measurements
b_2	s_2	Error due to differences in temperature from area measurement and testing

TABLE B-VI. - ELEMENTAL ERROR SOURCE EVALUATION FOR AREA MEASUREMENT SYSTEM

[Measured variable, diameter; range, all conditions.]

Source	Magnitude		Comments
	cm	in.	
b1	0.0025	.001	Instrument resolution
s1	.008	.003	Measurement repeatability
b2	0	0	Temperature effect accounted for in data reduction program
s2	0	0	

REFERENCES

1. Biesiadny, T.; Burkardt, L.; and Braithwaite, W: Uniform Engine Testing Program, Phase I: NASA Lewis Research Center Participation. NASA TM-82978, 1982.

2. Biesiadny, T.J.,et al.: Uniform Engine Testing Program, Phase VII: NASA Lewis Research Center, Phase VII. NASA TM-87272, 1986.

3. Abernathy, R.B.,et al.: Handbook, Uncertainty in Gas Turbine Measurements. AEDC-TR-73-5, 1973.

4. Uniform Engine Testing Program General Test Plan, AGARD Working Group No. 15, revised June 1983.

TABLE I. - PSL-3 DATA ACQUISITION TIME SUMMARY

Phase 1, scan and data acquisition, msec	0 to 100
Phase 2, engineering unit conversion, msec	100 to 150
Phase 3, limit checking and recording, msec	150 to 200
Phase 4, performance calculation, msec	200 to 600
Phase 5, display formatting, msec	600 to 700
Phase 6, display formatting, msec	700 to 750
Phase 7, graphic display, msec	750 to 850
Phase 8, spare, msec	850 to 1000

TABLE II. - PSL-4 DATA ACQUISITION TIME SUMMARY

Phase 1, data scan, acquisition, and transmission, msec	0 to 235
Phase 2, engineering unit conversion, msec	235 to 285
Phase 3, performance calculation, msec	285 to 625
Phase 4, limit checking, msec	625 to 660
Phase 5, history file write, msec	660 to 672
Phase 6, display output, msec	672 to 1070

TABLE III. - DATA ACQUISITION PARAMETERS

Measured variable	Total number of taps		Total scanning period (period per reading), sec		Number of scans per total period (scans per reading)		Number of dwells per reading	
	PSL-3	PSL-4	PSL-3	PSL-4	PSL-3	PSL-4	PSL-3	PSL-4
FS	[a] 4	[a] 4	20	30	20	20	1	1
WF	[b] 2	[b] 2			20		1	
P1	[c] 4	[c] 4			5		5	
PS1	4	4						
PAMB	4	4						
P2	20	20						
P7	36	36						
PS7	4	4						
TAIR	13	13			20		1	
T2	10	10						
T7	36	36						
NH	1	1						
NL	1	1						
PSEAL	4	4	20	30	5	20	5	1
PBOA1	4	4			5		5	
TM1	2	2			20		1	
TM7	4	4			20		1	

[a] Two load cells were used (FM, FP), each load cell consists of two bridges.

[b] Two flow meters were used.

[c] Four main stream pressures, plus four rakes of seven Pitots for boundary layer assessment.

TABLE IV. - MEASURED VARIABLE ERRORS

Measured variable					Error, percent of nominal value					
Name	Nominal value				Bias		Precision		Uncertainty	
	Condition	Unit	PSL-3	PSL-4	PSL-3	PSL-4	PSL-3	PSL-4	PSL-3	PSL-4
PS1	3	kPa	72.5	72.3	0.1076	0.1079	0.0303	0.0304	0.1683	0.1687
	6		71.2	71.6	.1320	.1313	.0309	.0307	.1938	.1927
	9		18.2	18.5	.3242	.3189	.1209	.1189	.5659	.5568
P1	3		84.0	83.2	.0655	.0661	.0262	.0264	.1179	.1190
	6		83.4	83.2	.0659	.0661	.0264	.0264	.1187	.1190
	9		20.8	21.0	.2644	.2619	.1058	.1048	.4760	.4714
P2	3		83.6	83.1	.0658	.0662	.0117	.0118	.0892	.0898
	6		83.1	82.9	.0662	.0663	.0118	.0118	.0898	.0900
	9		20.7	21.0	.2657	.2619	.0473	.0467	.3604	.3552
PS7	3		140.6	139.7	.0541	.3751	.0320	.0684	.1181	.5118
	6		139.7	138.4	.0544	.3786	.0322	.0690	.1188	.5166
	9		35.1	35.0	.2165	1.4971	.1282	.2729	.4729	2.0429
P7	3		152.9	152.8	.0497	.3429	.0098	.0208	.0693	.3846
	6		153.0	152.3	.0497	.3441	.0098	.0209	.0693	.3858
	9		38.6	38.5	.1969	1.3610	.0389	.0826	.2746	1.5262
PAMB	3		83.2	82.6	.0661	.0666	.0264	.0266	.1190	.1199
	6		63.9	63.7	.0861	.0863	.0344	.0345	.1549	.1554
	9		15.8	16.2	.3481	.3395	.1392	.1358	.6266	.6111
PSEAL	3		76.7	76.3	.0717	.0721	.0287	.0288	.1291	.1298
	6		68.0	68.3	.0809	.0805	.0324	.0322	.1456	.1449
	9		17.3	17.7	.3179	.3107	.1272	.1243	.5723	.5593
PBOAT	3		83.2	82.6	.0661	.0666	.0264	.0266	.1190	.1199
	6		63.9	63.7	.0861	.0863	.0344	.0345	.1549	.1554
	9	▼	15.8	16.2	.3481	.3395	.1392	.1358	.6266	.6111
TAIR	3	K	288.9	288.7	.4154	.4157	.0277	.0277	.4708	.4711
	6		288.9	288.5	.4154	.4159	.0277	.0277	.4708	.4714
	9		288.9	289.6	.4154	.4144	.0277	.0276	.4708	.4696
T2	3		288.9	288.7	0.4154	0.4157	0.0312	0.0312	0.4777	0.4780
	6		288.9	288.5	.4154	.4159	.0312	.0312	.4777	.4783
	9		288.9	289.6	.4154	.4144	.0312	.0311	.4777	.4765
T7	3		724.0	727.4	.3039	.3024	.0069	.0069	.3177	.3162
	6		725.0	718.4	.3034	.3062	.0069	.0070	.3172	.3202
	9	▼	805.0	801.2	.2733	.2746	.0062	.0062	.2857	.2871

TABLE IV. - Concluded.

Measured variable					Error, percent of nominal value					
Name	Nominal value				Bias		Precision		Uncertainty	
	Condition	Unit	PSL-3	PSL-4	PSL-3	PSL-4	PSL-3	PSL-4	PSL-3	PSL-4
TM1	3	K	295.3	291.5	0.4064	0.4117	0.0718	0.0727	0.5499	0.5571
	6	↓	287.9	287.5	.4168	.4174	.0736	.0737	.5641	.5649
	9	↓	287.9	289.5	.4168	.4145	.0736	.0732	.5641	.5610
TM7	3	↓	669.7	672.9	.3285	.3269	.0224	.0223	.3733	.3715
	6	↓	670.8	667.0	.3280	.3298	.0224	.0225	.3727	.3748
	9	↓	690.2	682.8	.3187	.3222	.0217	.0220	.3622	.3661
WF	3	g/s	547	551	.6216	.5626	.2925	.2904	1.2066	1.1434
	6	g/s	561	556	.6239	.5396	.2852	.2878	1.1943	1.1152
	9	g/s	164	163	.6098	.6135	.4878	.4908	1.5854	1.5951
FS	3	N	21 285	21 170	.3467	.3240	.1757	.1894	.6981	.7029
	6	N	18 750	18 200	.3936	.3769	.1995	.2269	.7925	.8308
	9	N	4 773	4 757	1.5462	1.4421	.7836	.7463	3.1133	2.9346
A1	3,6,9	m^2	.3711	.3711	.0073	.0073	.0221	.0221	.0514	0.0514
A8	3,6,9	↓	.2376	.2376	.0092	.0092	.0277	.0277	.0646	.0646
ASEAL	3,6,9	↓	.0335	.0335	.1191	.1191	.3592	.3592	.8375	.8775
ABOAT	3,6,9	↓	.1715	.1715	.0211	.0211	.0632	.0632	.1475	.1475
NL	3	rpm	5 252	5 249	.0152	.0152	0	0	.0152	.0152
	6	↓	5 335	5 311	.0150	.0151	↓	↓	.0150	.0151
	9	↓	5 402	5 373	.0148	.0149	↓	↓	.0148	.0149
NH	3	↓	8 874	8 884	.0135	.0135	↓	↓	.0135	.0135
	6	↓	8 874	8 887	.0135	.0135	↓	↓	.0135	.0135
	9	↓	8 862	8 872	.0135	.0135	↓	↓	.0135	.0135
LHV	3,6,9	J/N	43 234	43 234	.1180	.1180	.0680	.0680	.2540	.2540

TABLE V. - INFLUENCE COEFFICIENTS[a]

Measured variables			Performance parameter influence coefficients, percent/percent													
Name	Test cell	Test condition	WA1	FN	SFC	WA1RD	FNRD	SFCRD	WFRD	CD8	CG8	CV8	T7Q2	P7Q2	PS7Q2	NHRD	NLR
PS1	3	3	-2.711	-0.697	+0.703	-2.719	-0.815	+0.822	0	-2.706	-0.809	1.945	0	0	0	0	0
	4	3	-2.853	- .731	+ .736	-2.844	.870	+ .871		-2.841	- .862	2.038					
	3	6	-2.414	+ .393	- .396	-2.424	+ .392	- .394		-2.413	- .612	1.846					
	4	6	-2.596	+ .372	- .374	-2.399	+ .390	- .373		-2.593	- .699	1.946					
	3	9	-3.013	+ .465	- .465	-3.011	+ .447	- .454		-3.005	- .711	2.368					
	4	9	-3.124	+ .467	- .466	-3.124	+ .484	- .483		-3.116	- .742	2.453					
P1	3	3	3.568	2.086	-2.042	3.562	2.177	-2.130	0	3.565	2.165	-1.351	0	0	0	0	0
	4	3	3.696	2.150	-2.103	3.699	2.260	-2.209		3.688	2.244	-1.395					
	3	6	3.305	.834	- .831	3.293	.835	- .835		3.293	1.715	-1.527					
	4	6	3.470	.959	- .949	3.474	.965	- .957		3.462	1.864	-1.544					
	3	9	3.847	.805	- .792	3.852	.813	- .813		3.841	1.833	-1.933					
	4	9	3.953	.836	- .837	3.949	.831	- .820		3.945	1.887	-1.977					
P2	3	3	- .009	-4.724	4.960	- .996	-1.801	.824	- .989	- .005	- .003	.002	0	- .999	- .993	0	0
	4	3	.000	-4.367	4.567	- .990	-1.794	.819	- .990	.000	.000	.000		- .990	- .988		
	3	6	.000	-1.015	1.024	- .999	-1.784	.806	- .990	- .006	- .003	.002		- .993	- .987		
	4	6	.000	-1.021	1.026	- .989	-1.795	1.007	- .992	.000	.000	.000		- .990	- .988		
	3	9	- .007	- .912	.930	- .995	-1.752	.779	- .994	- .006	- .004	.003		- .991	- .998		
	4	9	.000	- .944	.941	- .991	-1.762	.785	- .993	.000	.000	.000		- .986	- .988		
PS7	3	3	0	0	0	0	0	0	0	0	0	0	0	.999	0	0	0
	4	3												.999			
	3	6												1.010			
	4	6												1.000			
	3	9												1.003			
	4	9												1.000			
P7	3	3	0	0	0	0	0	0	0	-1.023	-1.749	- .732	0	0	1.001	0	0
	4	3								-1.013	-1.729	- .724			.995		
	3	6								-1.000	-1.467	- .471			.998		
	4	6								-1.000	-1.472	- .477			1.001		
	3	9								-1.002	-1.460	- .461			.996		
	4	9								-1.002	-1.478	- .481			1.003		
PAMB	3	3	0	-2.770	-2.850	0	-1.071	1.061	0	.023	-1.082	-1.110	0	0	0	0	0
	4	3		-2.410	-2.470		-1.065	1.055		.013	-1.097	-1.110					
	3	6		- .824	.831		-1.057	1.065		.000	- .704	.704					
	4	6		- .845	.853		-1.072	1.081		.000	- .712	- .713					
	3	9		- .841	.852		-1.010	1.044		.000	- .693	- .692					
	4	9		- .872	.872		-1.032	1.044		.000	- .712	- .711					
PSEAL	3	3	0	.036	- .035	0	.033	- .033	0	0	.033	.033	0	0	0	0	0
	4	3		.037	- .035		.033	- .033			.033	.033					
	3	6		.055	- .058		.058	- .058			.037	.036					
	4	6		.057	- .057		.059	- .057			.038	.037					
	3	9		.063	- .052		.054	- .060			.037	.038					
	4	9		.054	- .060		.064	- .060			.038	.039					
PBOA1	3	3	0	.613	- .608	0	.579	- .577	0	0	.578	.577	0	0	0	0	0
	4	3		.613	- .609		.577	- .574			.575	.574					
	3	6		.571	- .569		.571	- .576			.367	.367					
	4	6		.581	- .575		.581	- .581			.371	.371					
	3	9		.545	- .542		.545	- .514			.361	.360					
	4	9		.557	- .561		.566	- .561			.372	.377					
1A1R	3	3	- .499	.031	- .03	- .502	0	0	0	- .496	0	.499	0	0	0	0	0
	4	3	- .502	.035	- .034	- .495	0	0		- .496	.001	.499					
	3	6	- .493	.279	- .280	- .504	.277	- .278		- .496	.001	.499					
	4	6	- .498	.282	- .278	- .490	.282	- .287		- .495	.001	.499					
	3	9	- .497	.259	- .249	- .493	.250	- .265		- .495	.001	.499					
	4	9	- .497	.252	- .259	- .499	.256	- .258		- .496	.001	.497					

[a]For all test conditions and test cells, measured variables ABOA1, NL, NH, AND LHV had influence coefficients of zero except for the following performance parameters: NL = 1.0 for NLR; NH = 1.0 for NHRD; LHV = 1.0 for SFCRD and WFRD.

TABLE V. - Concluded.

Measured variables			Performance parameter influence coefficients, percent/percent													
Name	Test cell	Test condition	WA1	FN	SFC	WA1RD	FNRD	SFCRD	WFRD	CD8	CG8	CV8	T7Q2	P7Q2	PS7Q2	NHRD	NLR
T2	3	3	0.000	-0.027	0.026	0.502	0.004	-0.500	-0.495	0.007	0.003	-0.004	-0.990	0	0	-0.496	-0.495
	4	3	.000	- .035	.034	.504	0.000	- .497	- .496	0.000	0.000	0.000	- .988			- .497	- .498
	3	6	.009	- .276	.270	.504	.275	- .221	- .497	.007	.005	- .003	- .993			- .496	- .497
	4	6	.000	- .284	.278	.498	- .280	- .220	- .497	0.000	0.000	0.000	- .987			- .497	- .498
	3	9	.007	- .250	.258	.508	- .259	- .240	- .497	.008	.004	- .004	.991			- .497	- .496
	4	9	.000	- .261	.250	.495	- .256	- .242	- .496	0.000	0.000	0.000	- .990			- .496	- .496
T7	3	3	0	0	0	0	0	0	0	.522	.011	- .509	1.002	0	0	0	0
	4	3								.522	.013	- .507	1.001				
	3	6								.522	.010	- .509	1.000				
	4	6								.522	.010	- .509	1.003				
	3	9								.526	.012	- .511	.998				
	4	9								.525	.011	- .511	1.001				
TM1	3	3	.009	.002	- .001	.009	.002	- .001	0	.010	.001	- .010	0	0	0	0	0
	4	3	.009	.002	- .001	.009	.002	- .001		.010	.002	- .008					
	3	6	.009	.000	.000	.009	.000	.000		.009	.004	- .006					
	4	6	.009	.000	.000	.009	.002	.000		.009	.004	- .006					
	3	9	.007	.000	.000	.011	.000	.000		.009	.003	- .006					
	4	9	.011	.000	.000	.007	.000	- .009		.009	.003	- .006					
TM7	3	3	0	0	0	0	0	0	0	-0.015	-0.016	0	0	0	0	0	0
	4	3								- .016	- .015						
	3	6								- .016	- .015						
	4	6								- .016	- .015						
	3	9								- .016	- .017						
	4	9								- .016	- .016						
WF	3	3	0	0	1.000	0	0	1.000	1.009	.012	0	- .011	0	0	0	0	0
	4	3			.999			.999	1.002	.012	.002	- .011					
	3	6			.995			.998	.999	.011	.001	- .011					
	4	6			.997			.995	.999	.012	.002	- .011					
	3	9			1.007			1.001	1.002	.016	.001	- .013					
	4	9			.993			.992	1.001	.015	.001	- .013					
FS	3	3	0	.915	- .906	0	.867	- .859	0	0	.862	.858	0	0	0	0	0
	4	3		.918	- .909		.863	- .855			.839	.858					
	3	6		.978	- .975		.980	- .969			.628	.627					
	4	6		.968	- .958		.970	- .967			.619	.619					
	3	9		.957	- .947		.956	- .950			.633	.634					
	4	9		.962	- .958		.968	- .958			.637	.638					
A1	3	3	.999	.099	- .099	.996	.152	- .151	0	.998	.148	- .841	0	0	0	0	0
	4	3	.996	.096	- .096	.999	.155	- .155			.154	- .837					
	3	6	1.004	.009	- .010	.999	.012	- .010			.364	- .627					
	4	6	1.005	.019	- .019	1.006	.021	- .019			.373	- .619					
	3	9	.998	.027	- .026	1.002	.027	- .026			.355	- .636					
	4	9	1.001	.018	- .026	.998	.027	- .026			.353	- .639					
A8	3	3	0	0	0	0	-0.004	0.004	0	-0.999	-0.991	0.011	0	0	0	0	0
	4	3					- .005	.005		- .998	- .989	.010					
	3	6					.000	.000		-1.000	- .990	.010					
	4	6					.000	.000		-1.000	- .989	.010					
	3	9					- .009	- .009		-1.002	- .990	.013					
	4	9					- .009	- .009		-1.002	- .990	.012					
ASEAL	3	3	0	- .013	.013	0	- .013	.013	0	0	- .014	- .013	0	0	0	0	0
	4	3		- .014	.014		- .013	.013			- .013	- .013					
	3	6		+ .009	- .019		+ .012	- .019			+ .007	.007					
	4	6		+ .012	- .009		+ .012	- .019			+ .008	.008					
	3	9		+ .018	- .009		+ .009	- .017			+ .009	.010					
	4	9		+ .009	- .017		+ .018	- .017			+ .008	.029					

TABLE VI. - PERFORMANCE PARAMETER ERRORS[a]

Performance parameter			Error, percent of reading		
Name	Test cell	Test condition	Bias	Precision	Uncertainty
WA1	3	3	0.43	0.13	0.68
	4	3	.45	.13	.71
	3	6	.44	.12	.67
	4	6	.46	.12	.71
	3	9	1.43	.55	2.52
	4	9	1.45	.56	2.57
FN	3	3	.51	.19	.90
	4	3	.48	.20	.88
	3	6	.44	.20	.84
	4	6	.42	.22	.87
	3	9	1.57	.77	3.11
	4	9	1.48	.74	2.96
SFC	3	3	.81	.35	1.51
	4	3	.74	.35	1.45
	3	6	.76	.35	1.45
	4	6	.68	.36	1.41
	3	9	1.67	.91	3.49
	4	9	1.60	.88	3.37
WA1RD	3	3	.48	.13	.74
	4	3	.49	.13	.76
	3	6	.49	.12	.73
	4	6	.49	.12	.73
	3	9	1.47	.55	2.56
	4	9	1.49	.56	2.61
FNRD	3	3	.37	.17	.71
	4	3	.36	.18	.72
	3	6	.45	.20	.86
	4	6	.44	.23	.89
	3	9	1.63	.78	3.18
	4	9	1.55	.75	3.06
SFCRD	3	3	.75	.34	1.44
	4	3	.70	.35	1.39
	3	6	.77	.35	1.48
	4	6	.68	.37	1.42
	3	9	1.69	.91	3.51
	4	9	1.61	.89	3.39

[a]Performance parameters NHRD and NLRD shared bias, precision, and uncertainty errors of 0.21, 0.02, and 0.24 percent of readings for all conditions and cells.

TABLE VI. - Concluded.

Performance parameter			Error, percent of reading		
Name	Test cell	Test condition	Bias	Precision	Uncertainty
WFRD	3	3	0.67	0.30	1.28
	4	3	.62	.30	1.21
	3	6	.67	.29	1.26
	4	6	.59	.30	1.19
	3	9	.71	.50	1.70
	4	9	.71	.50	1.70
CD8	3	3	.46	.13	.72
	4	3	.58	.14	.86
	3	6	.47	.12	.71
	4	6	.60	.13	.85
	3	9	1.44	.55	2.54
	4	9	1.99	.56	3.12
CG8	3	3	.36	.17	.70
	4	3	.68	.18	1.04
	3	6	.30	.14	.58
	4	6	.58	.16	.90
	3	9	1.18	.55	2.29
	4	9	2.29	.55	3.39
CV8	3	3	.46	.17	.81
	4	3	.52	.18	.89
	3	6	.45	.15	.74
	4	6	.48	.16	.80
	3	9	1.40	.62	2.64
	4	9	1.51	.61	2.73
T7Q2	3	3	.51	.03	.58
	4	3	↓	↓	.57
	3	6	↓	↓	.58
	4	6	↓	↓	.58
	3	9	.49	↓	.56
	4	9	.49	↓	.56
P7Q2	3	3	.08	.02	.11
	4	3	.35	.02	.39
	3	6	.08	.02	.11
	4	6	.35	.02	.40
	3	9	.33	.06	.45
	4	9	1.39	.09	1.58
PS7Q2	3	3	.08	.03	.15
	4	3	.38	.07	.52
	3	6	.09	.03	.15
	4	6	.38	.07	.52
	3	9	.34	.14	.62
	4	9	1.52	.28	2.07

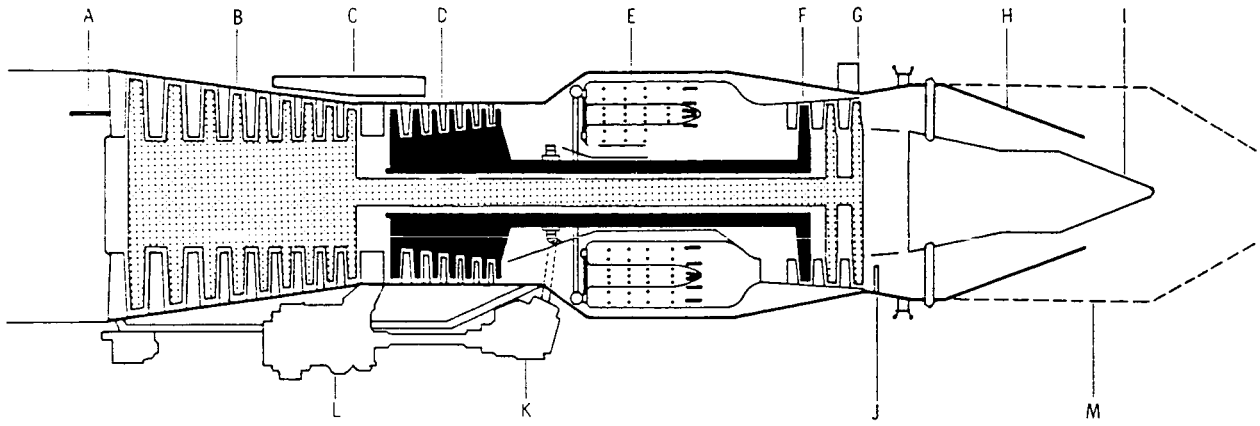

A. EPR PROBE (INLET PRESSURE)
B. LOW PRESSURE COMPRESSOR
C. OIL SUPPLY TANK
D. HIGH PRESSURE COMPRESSOR
E. BURNER CANS
F. FIRST STAGE TURBINE
G. SECOND AND THIRD STAGE TURBINE
H. NOZZLE
I. TAIL CONE
J. EPR PROBE (EXHAUST PRESSURE)
K. ACCESSORY DRIVE ELBOW
L. ACCESSORY DRIVE HOUSING
M. MODIFIED TAILPIPE AND NOZZLE ASSEMBLY

(A) J57 ENGINE SCHEMATIC.

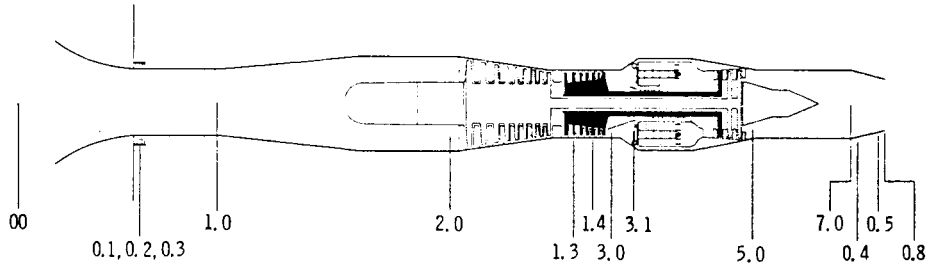

0.0	INLET PLENUM
0.1, 0.2, 0.3	LABYRINTH SEAL
1.0	AIRFLOW STATION
2.0	ENGINE OR LPC INLET
1.3	LPC BLEED ANNULUS
1.4	LPC BLEED PORT
3.0	COMBUSTOR INLET
3.1	COMBUSTER DIFFUSER EXIT
5.0	LPT EXIT
7.0	EXHAUST NOZZLE INLET
0.4, 0.5, 0.8	EXHAUST NOZZLE (EXTERNAL)

(B) INSTRUMENTATION LOCATIONS.

FIGURE 1. - ENGINE SCHEMATIC AND INSTRUMENTATION LOCATIONS.

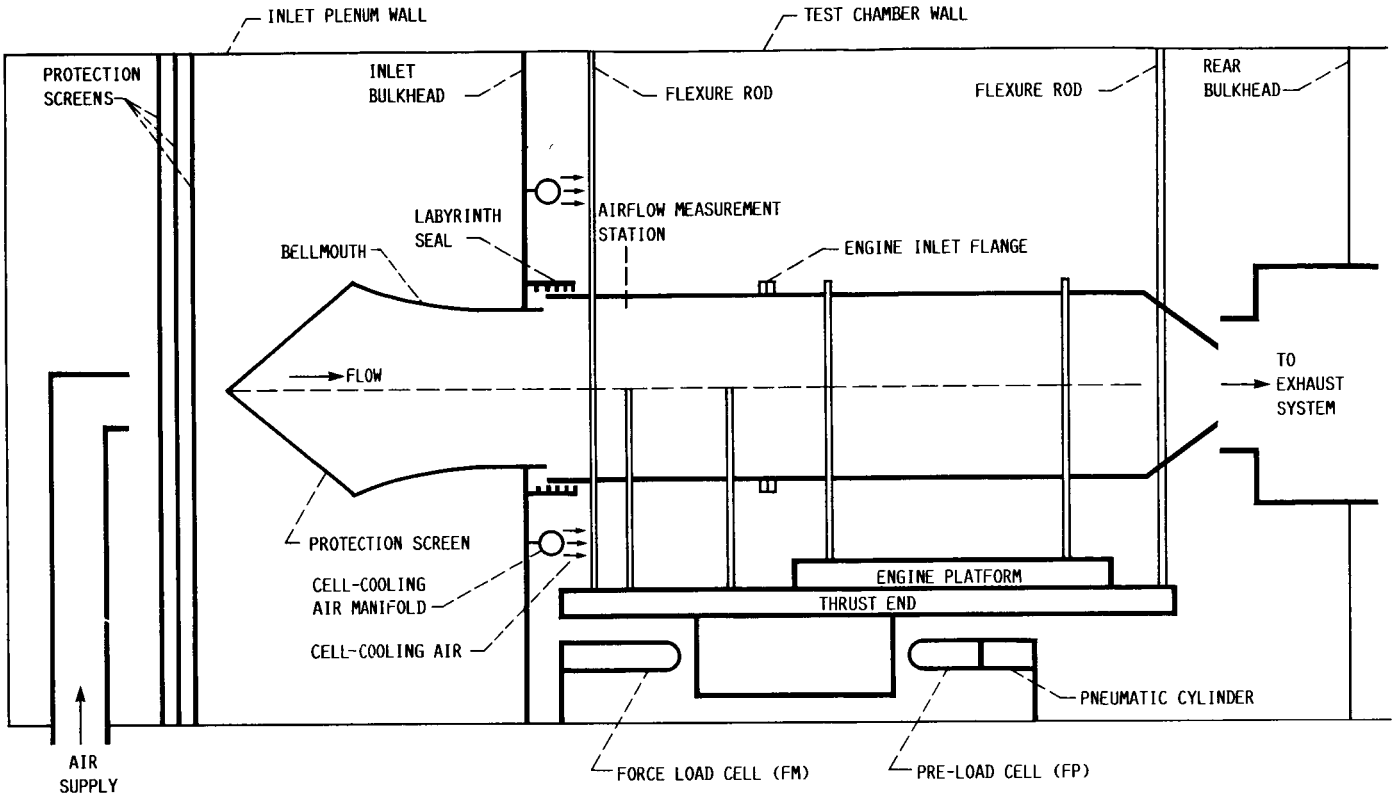

FIGURE 2. - SCHEMATIC OF ENGINE INSTALLATION IN THE LEWIS NASA ALTITUDE TEST FACILITY.

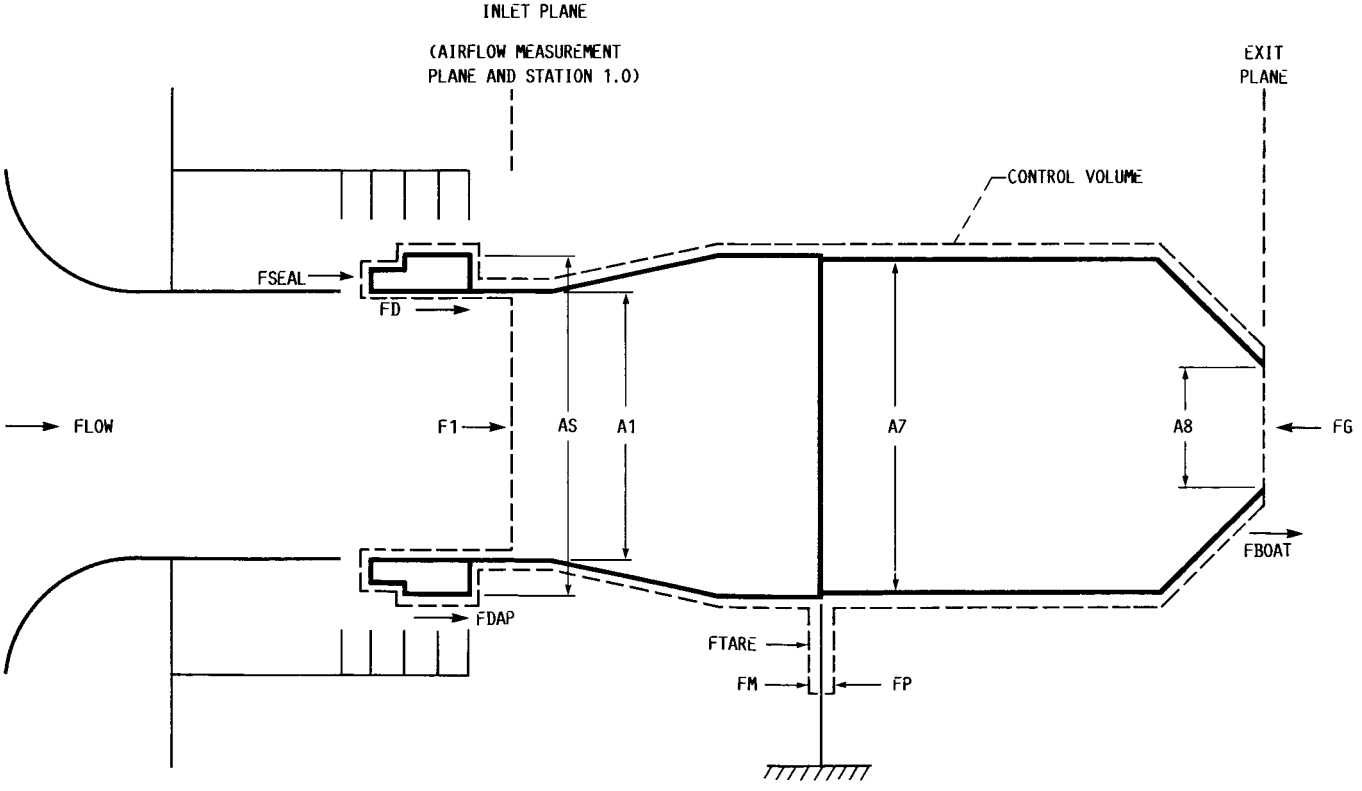

FIGURE 3. - FORCES CONSIDERED IN A THRUST EVALUATION.

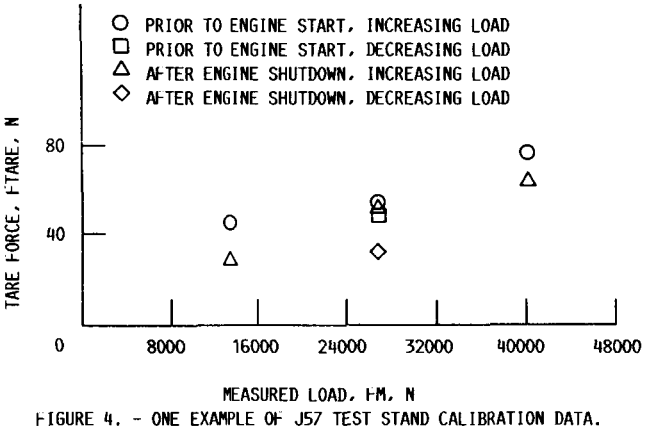

FIGURE 4. - ONE EXAMPLE OF J57 TEST STAND CALIBRATION DATA.

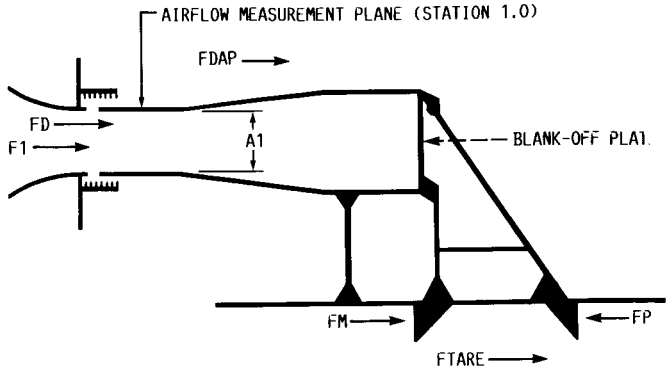

(A) FDAP CALIBRATION SCHEMATIC.

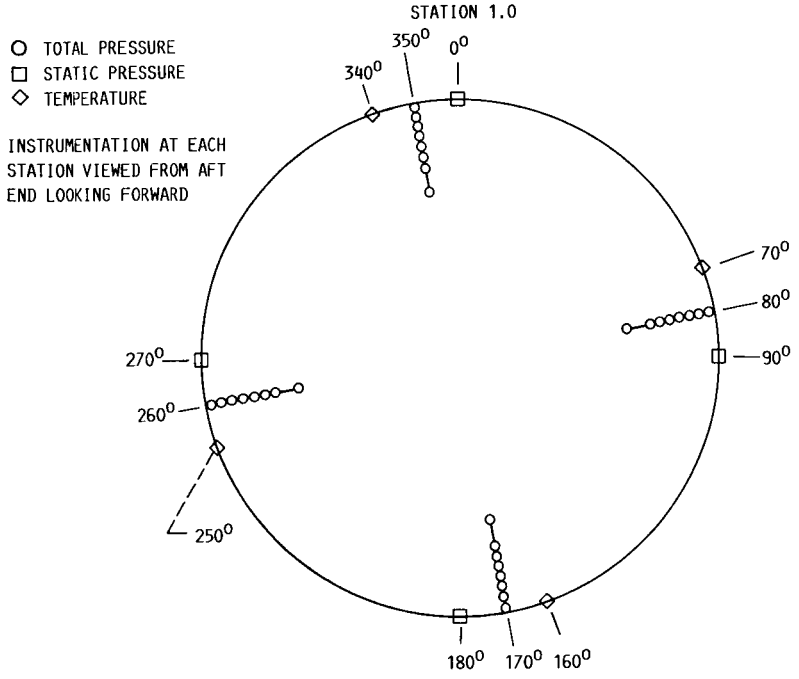

(B) AIRFLOW MEASUREING STATION INSTRUMENTATION.

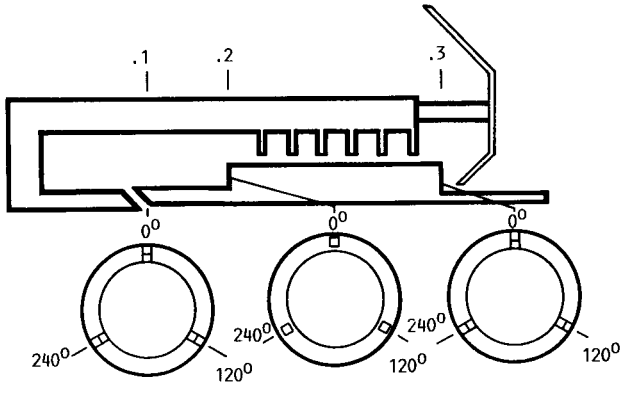

STATION 0.1, 0.2, 0.3

(C) LABYRINTH SEAL INSTRUMENTATION.

FIGURE 5. - FADP CALIBRATION SCHEMATIC AND INSTRUMENTATION.

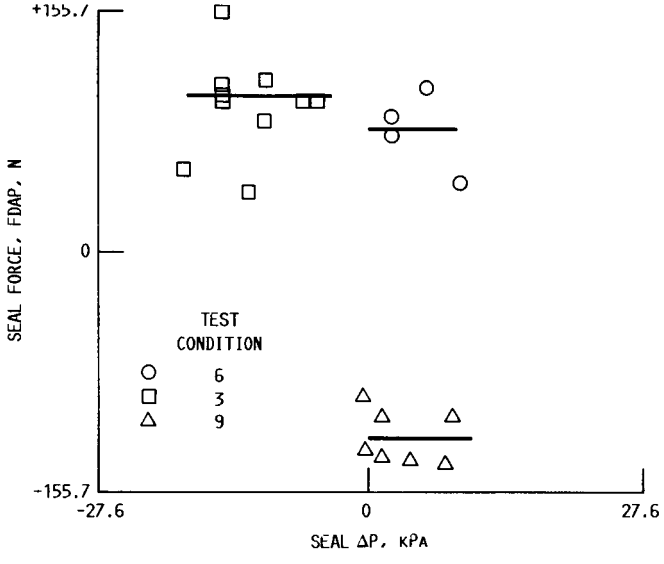

FIGURE 6. - FDAP CALIBRATION DATA.

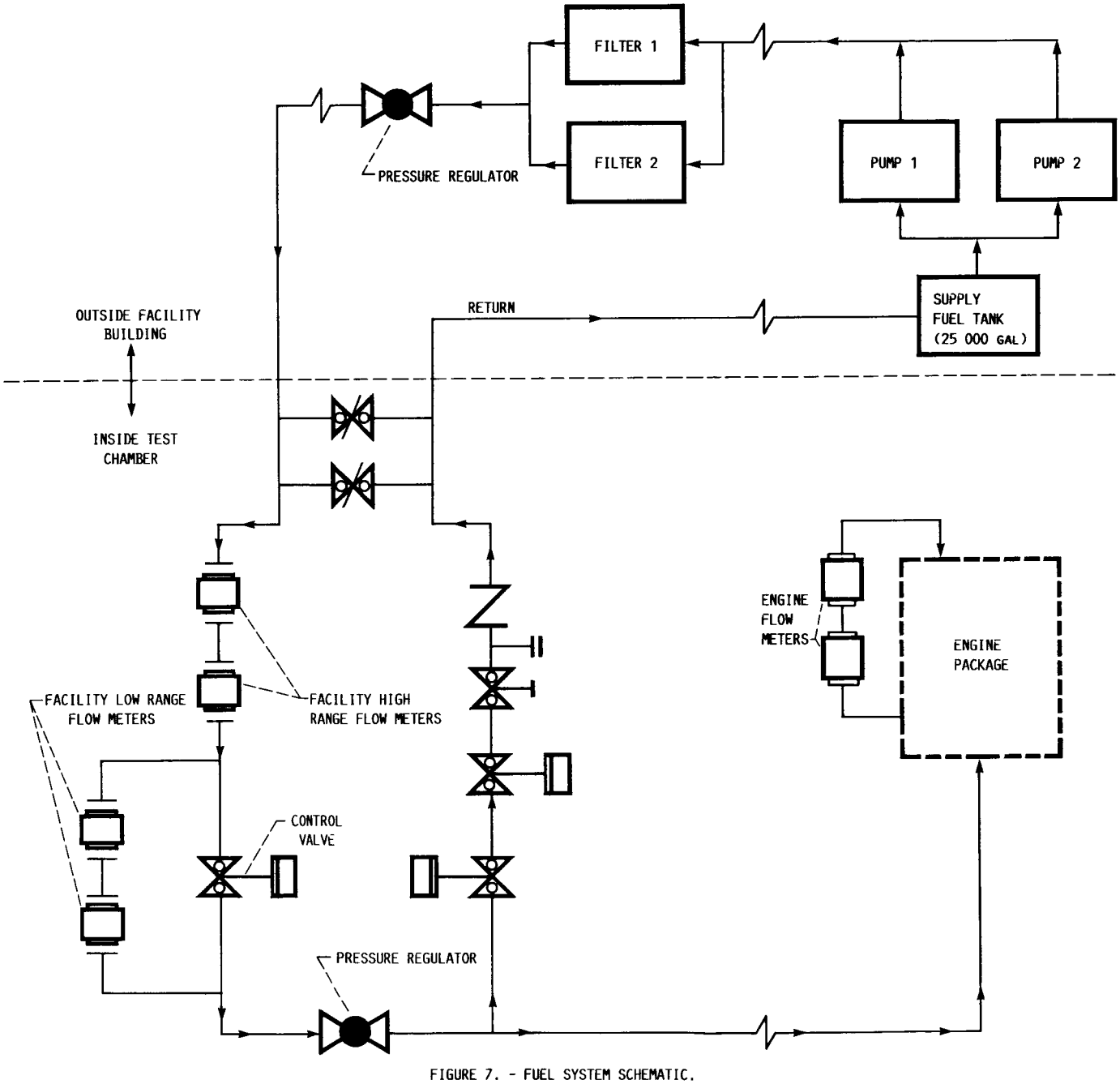

FIGURE 7. - FUEL SYSTEM SCHEMATIC.

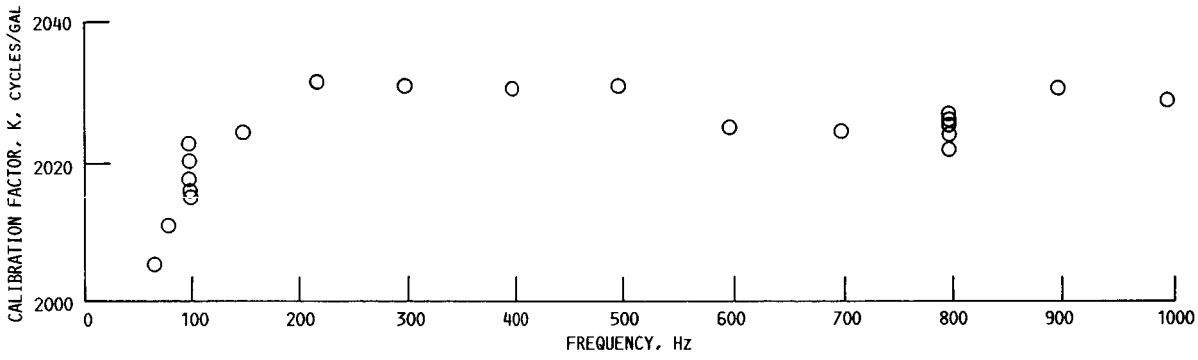

FIGURE 8. - TYPICAL FUEL FLOW METER CALIBRATION DATA.

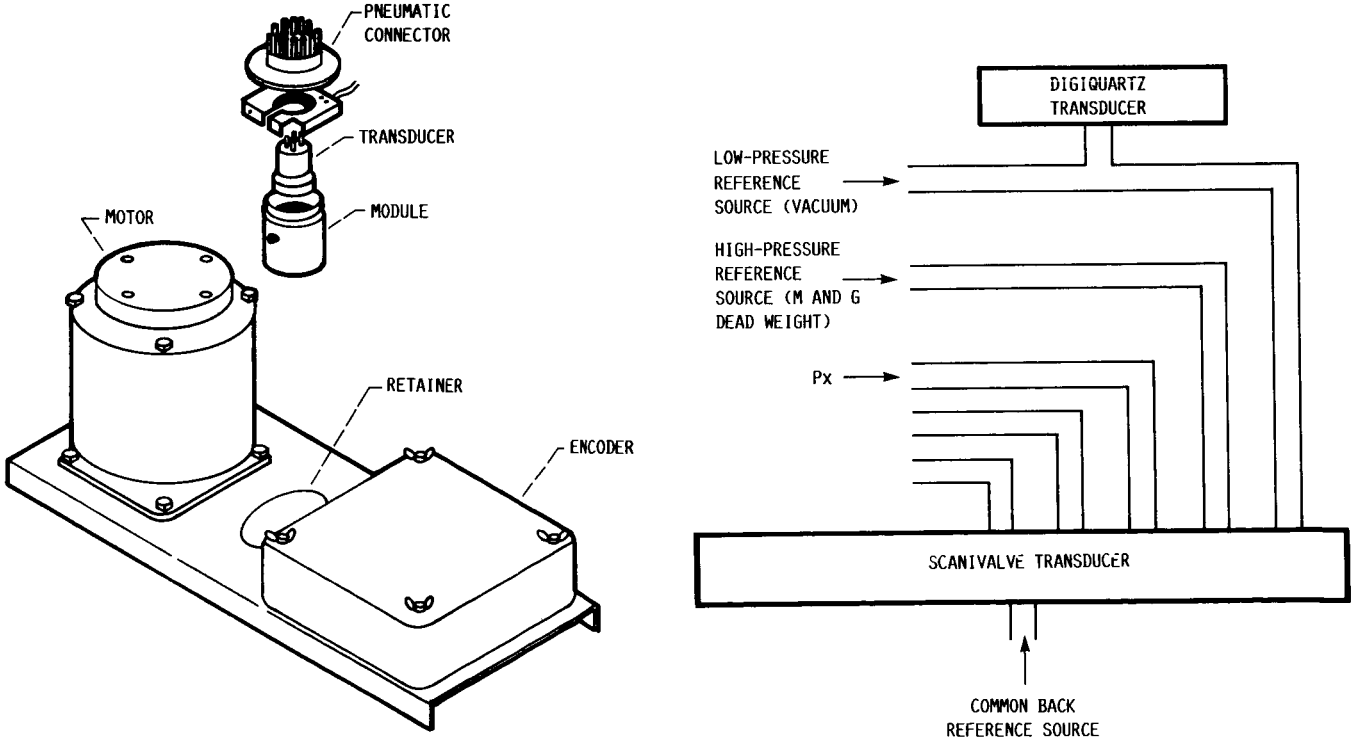

(A) SCANIVALVE SYSTEM.

(B) SCHEMATIC OF PSL-3 PRESSURE MEASUREMENT CALIBRATION SYSTEM.

FIGURE 9. - SCHEMATIC OF PSL-3 MULTIPLE PRESSURE SCANNING SYSTEM.

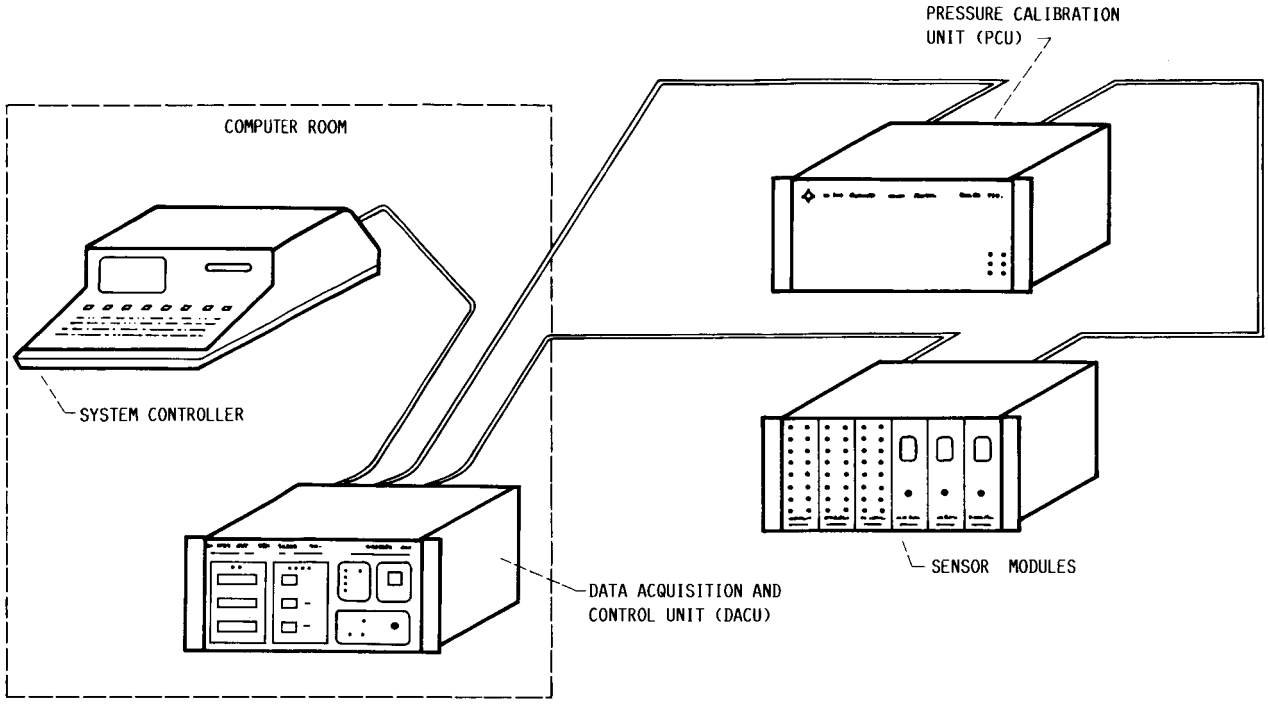

FIGURE 10. - PSL-4 PRESSURE SYSTEM FUNCTIONAL DIAGRAM.

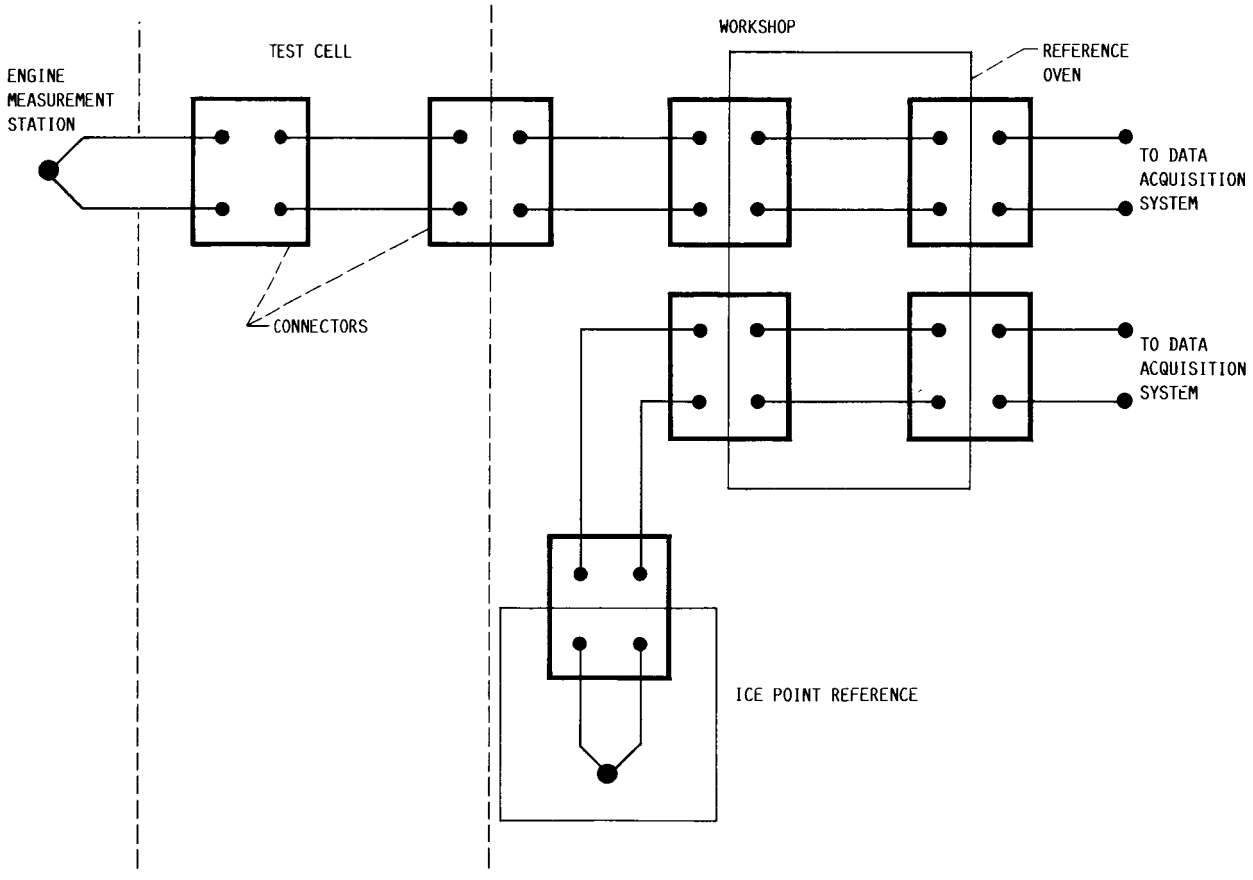

FIGURE 11. - SCHEMATIC OF TEMPERATURE MEASUREMENT SYSTEM.

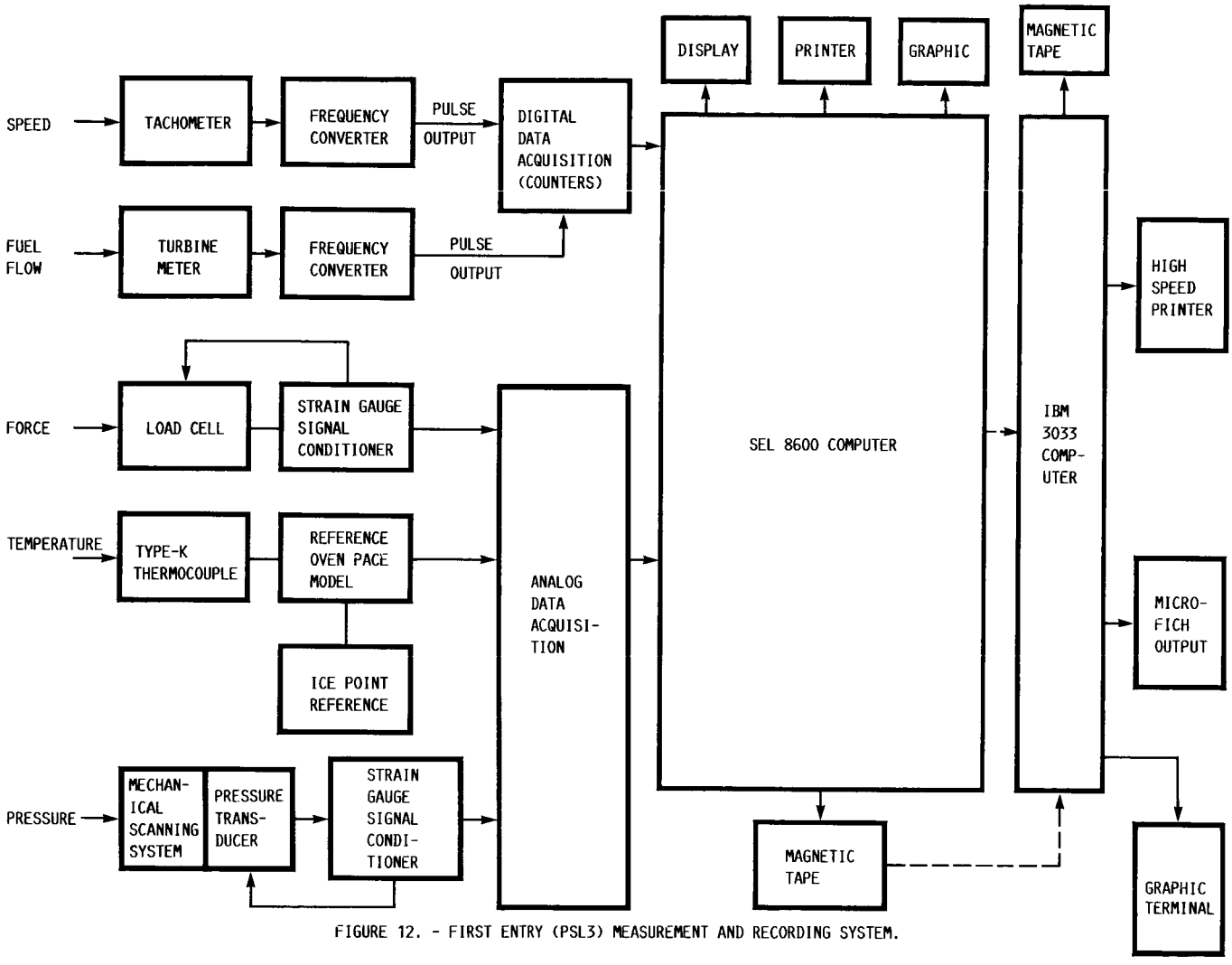

FIGURE 12. - FIRST ENTRY (PSL3) MEASUREMENT AND RECORDING SYSTEM.

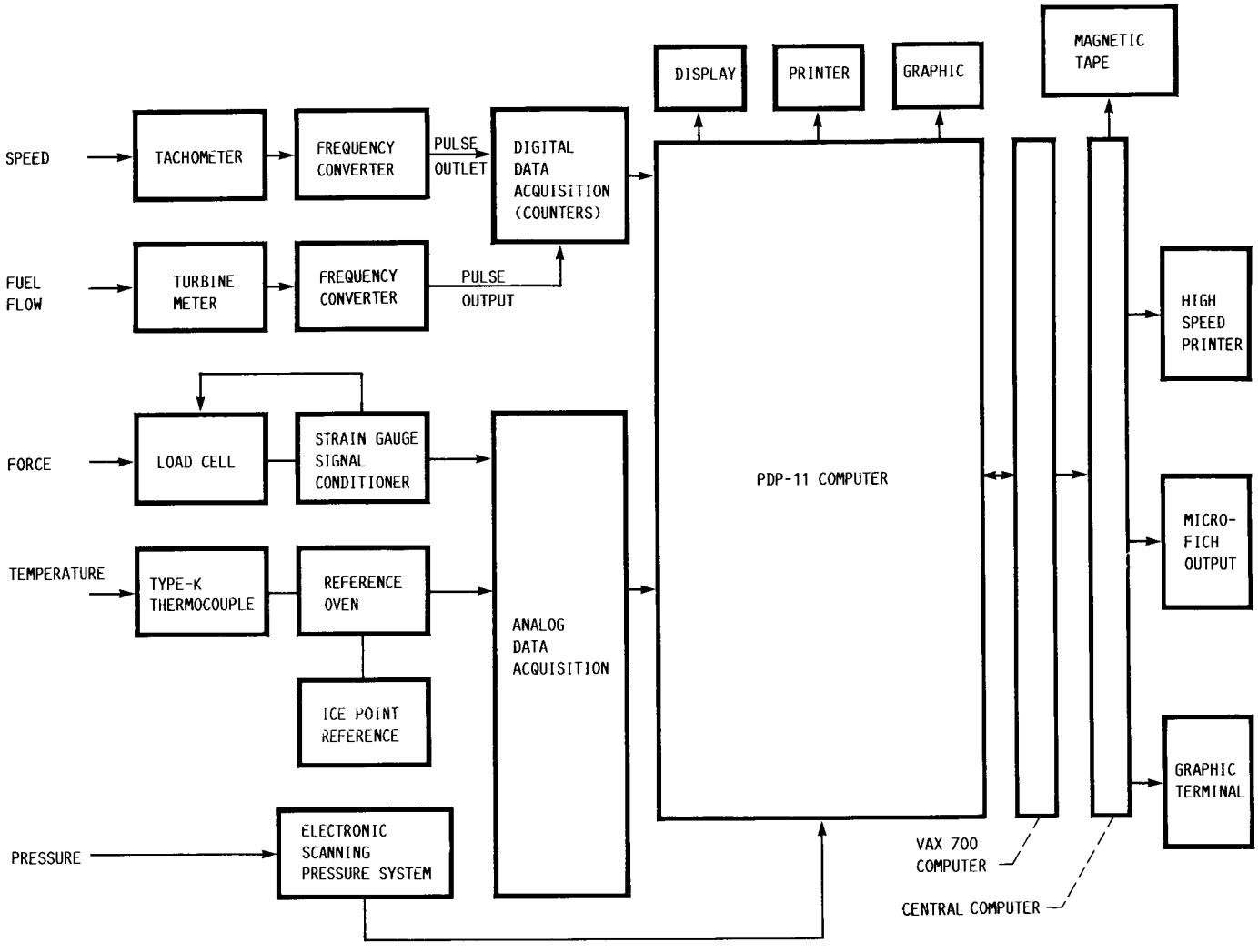

FIGURE 13. - SECOND ENTRY (PSL-4) MEASUREMENT AND RECORDING SYSTEM.

1. Report No.	2. Government Accession No.	3. Recipient's Catalog No.
NASA TM-88943		

4. Title and Subtitle	5. Report Date
Measurement Uncertainty for the Uniform Engine Testing Program Conducted at NASA Lewis Research Center	May 1987
	6. Performing Organization Code: 505-65-3B
7. Author(s): Mahmood Abdelwahab, Thomas J. Biesiadny, and Dean Silver	8. Performing Organization Report No.: E-3234
	10. Work Unit No.
9. Performing Organization Name and Address: National Aeronautics and Space Administration, Lewis Research Center, Cleveland, Ohio 44135	11. Contract or Grant No.
	13. Type of Report and Period Covered: Technical Memorandum
12. Sponsoring Agency Name and Address: National Aeronautics and Space Administration, Washington, D.C. 20546	14. Sponsoring Agency Code

15. Supplementary Notes

Mahmood Abdelwahab and Thomas J. Biesiadny, NASA Lewis Research Center; Dean Silver, Air Force Systems Command Liaison Office, Lewis Research Center, Cleveland, Ohio 44135.

16. Abstract

An uncertainty analysis was conducted to determine the bias and precision errors and total uncertainty of measured turbojet engine performance parameters. The engine tests were conducted as part of the Uniform Engine Test Program which was sponsored by the Advisory Group for Aerospace Research and Development (AGARD). With the same engines, support hardware, and instrumentation, performance parameters were measured twice, once during tests conducted in test cell number 3 and again during tests conducted in test cell number 4 of the NASA Lewis Propulsion Systems Laboratory. The analysis covers 15 engine parameters, including engine inlet airflow, engine net thrust, and engine specific fuel consumption measured at high rotor speed of 8875 rpm. Measurements were taken at three flight conditions defined by the following engine inlet pressure, engine inlet total temperature, and engine ram ratio: (1) 82.7 kPa, 288 K, 1.0, (2) 82.7 kPa, 288 K, 1.3, and (3) 20.7 kPa, 288 K, 1.3. In terms of bias, precision, and uncertainty magnitudes, there were no differences between most measurements made in test cell numbers 3 and 4. The magnitude of the errors increased for both test cells as engine pressure level decreased. Also, the level of the bias error was two to three times larger than that of the precision error.

17. Key Words (Suggested by Author(s))	18. Distribution Statement
Jet engine; Error; Uncertainty; Precision; Bias; Engine performance parameters	Unclassified - unlimited STAR Category 07

19. Security Classif. (of this report)	20. Security Classif. (of this page)	21. No. of pages	22. Price*
Unclassified	Unclassified	52	A04

*For sale by the National Technical Information Service, Springfield, Virginia 22161